RESEARCH REPORT UMP GRANT
Laporan Prestasi Skim Geran UMP

Final	√	Progress		*Progress Period :* _____	√

Please tick

PROJECT DETAILS *(Keterangan Projek)*

A	**Grant No**	RDU1403126
	Faculty/CoE	FTKMA
	Project Title	IMPACT BIODIESEL FUEL CHARACTERISTICS ON ULTRA-LOW EMISSION HOMOGENEOUS CHARGE COMPRESSION IGNITION ENGINE
	Project Leader	PROF. TS. DR. MD MUSTAFIZUR RAHMAN
	Project Member	1. DR. MUHAMAD MAT NOOR, FTKMA 2. PM DR ABDUL ADAM ABDULLAH FTKMA 3. PROF. DATO DR ROSLI ABU BAKAR, FTKMA 4. PROF. DR. RIZALMAN MAMAT, FTKMA 5. PM DR KUMARAN KADIRGAMA, FTKMA 6. PM DR DEVARAJAN RAMASAMY, FTKMA

PROJECT ACHIEVEMENT *(Pencapaian Projek)*

B

ACHIEVEMENT PERCENTAGE				
Project progress according to milestones achieved up to this period	**0 - 25%**	**26 - 50%**	**51 - 75%**	**76 - 100%**
Percentage (please state %)				100%

EXPENDITURE *(Perbelanjaan)*

C

Budget Approved *Peruntukan diluluskan*	**Amount Spent** *Jumlah Perbelanjaan*	**Balance** *Baki*	**% of Amount Spent** *Peratusan Belanja*
RM38,575.00	**RM30,916.00**	**RM7659.00**	**80.15 %**

RESEARCH OUTPUT *(Output Penyelidikan)*

D

NO OF PUBLICATION

KPI FOR NO OF PUBLICATION

	ISI	Scopus	Index Proceedings	Others
KPI	**1**	**2**	**1**	
Achievement	**2**	**1**	**1**	

The contribution of funder (UMP, MOHE, MOSTI, Industry etc.) as the fund provider must be acknowledged at all times in all forms of publications. Please state the grant number (RDU/UIC) and

grant name.

	ISI	Scopus
Number of articles/ manuscripts/books *(Please attach the First Page of Publication)*	1. M.M. Hasan and M.M. Rahman. 2016. Homogeneous Charge Compression Ignition Combustion: Advantages over Compression Ignition Combustion, Challenges and Solutions. Renewable and Sustainable Energy Reviews. 57: 282-291, (SCI Index, Q1, IF =6.798) 2. Hasan, M.M., Rahman, M.M., Nomani Kabir, M., Abdullah, A.A. 2017. Numerical Study on the Combustion and Performance Characteristics of an HCCI Engine Resulting from the Autoignition of Gasoline Surrogate Fuel. Journal of Energy Engineering, 143(5):4017049 (WoS Index, IF: 1.346, Q3)	1. M.M. Hasan, M.M. Rahman, and K. Kadirgama. A Review on Homogeneous Charge Compression Ignition Engine Performance using Biodiesel–Diesel Blend as a Fuel. International Journal of Automotive and Mechanical Engineering, 11:2199-2211. (Scopus Index)

	International	National
Conference Proceeding *(Please attach the First Page of Publication)*	1. H.Hanafi,, M.M.Hasan,, M.M.Rahman, M.M.Noor, K.Kadirgama and D. Ramasamy. 2016. Numerical modeling on homogeneous charge compression ignition combustion engine fueled by diesel-ethanol blends. MATEC Web of Conferences 74, 00037, 1-9.	1. 2.

HUMAN CAPITAL DEVELOPMENT

KPI FOR HUMAN CAPITAL DEVELOPMENT

	PhD Student	Master Student
KPI		**1**
Achievement		**1**

Human Capital Development	**Number**				**Others** (please specify)
	On-going		**Graduated**		
Citizen	Malaysian	Non Malaysian	Malaysian	Non Malaysian	
PhD Student				1	
Masters Student					
Undergraduate Student					
Total				1	

Name of Student:	MOHAMMAD MEHEDI HASSAN
ID Matric No:	MMM14004
Faculty:	FACULTY OF MECHANICAL AND AUTOMOTIVE ENGINEERING TECHNOLOY
Thesis title:	NUMERICAL INVESTIGATION ON COMBUSTION, PERFORMANCE AND EMISSIONS CHARACTERISTICS IN HOMOGENEOUS CHARGE COMPRESSION IGNITION ENGINE
Graduation Year:	2016

INTELECTUAL PROPERTIES

KPI FOR INTELECTUAL PROPERTIES

Patent, Copyright, Trademark,Industrial Design: _____

Patent, Copyright, Trademark, Industrial Design ect	

OTHERS

KPI FOR OTHERS

Prototype, Technology,Collaborations etc: _____

Prototype, Technology, Collaborations etc	

ASSET *(Aset)*

E

Bil	**Peralatan** *(Equipment)*	**Model**	**No Daftar Aset** *(Asset Tagging No)*	**Amount** (RM)	**Lokasi** *(Location)*

PRODUCT DESCRIPTION FOR UMP R&D DIRECTORY (SHORT & BRIEF) *Only for Final Report*

F NOT APPLICABLE

PRODUCT PICTURE FOR UMP R&D DIRECTORY *Only for Final Report*

G NOT APPLICABLE

SUMMARY OF RESEARCH FINDINGS (*Ringkasan Penemuan Projek Penyelidikan)*

H Homogeneous charge compression ignition (HCCI) engine has been an active research area due to its potential for high fuel conversion efficiency and extremely low emissions of particulate matter and oxides of nitrogen (NO_x). However, the operational range using HCCI combustion in terms of speed and load is restricted because the start of combustion (SOC) and the heat release rate cannot be controlled directly. Depending only on the thermal history and chemical behavior of the cylinder contents, SOC is manipulated by precise manipulation of these variables through methods such as intake temperature and pressure conditioning, fuel blending, variable cylinder geometry, and variable valve timings. In order to design an engine for extended operational range as well as various fuels and blends of fuels, accurate models are needed which are able to model both combustion and performance. The objectives of this study are to impact biodiesel fuel characteristics on ultra-low emission homogeneous charge compression ignition engine. In this study, a zero dimensional single-zone numerical simulation with reduced fuel chemistry of various fuels and blends of fuels was developed and validated. It is known for its advantage in reducing computational time compared with a multi-dimensional Computational Fluid Dynamics approach. The main focus of the study is to obtain an improved result for the zero-dimensional model, while the experimental results were used for the purpose of validation. The obtained results show good agreement with the experimental published results and capture important combustion phase trends as engine parameters are varied with a maximum percentage of error which is less than 6% for diesel HCCI and 4% for gasoline HCCI. The combustion phase advances and the combustion duration shorten with the increase of intake charge temperature and the decrease of the engine speed for both diesel and gasoline HCCI. The maximum load successfully increased with increasing the intake pressure. The highest load in this study was 11.27 bar in IMEPg at the condition of 200 kPa in intake air pressure and 333 K in intake air temperature for diesel HCCI and 10.86 bar in IMEPg at the condition of 200 kPa in intake air pressure and 393 K in intake air temperature for gasoline HCCI. It is found that the intake air pressure gives the most sensitive influence on HCCI combustion and performance characteristics. For various fuel blends, thermal efficiency was increased by about 17.71% with Bu30 compared to n-heptane at 393 K intake temperature. IMEP decreased at all intake temperatures with n-heptane. Very low amount of NO_x emissions were found with test fuels which is less than 2.5 ppm. NO_x emissions were increased with the increase of intake temperature. It is also seen that carbon monoxide (CO) emissions were increased with the increase of alcohol in the test fuels. Maximum CO emissions were found as 0.47% with E30 at 313 K intake temperature. Moreover, higher hydrocarbon (HC) emissions were obtained especially at lower intake temperature when ethanol was used as an additive fuel. Maximum HC emissions were found as 159.6 ppm with E30 test fuel at 313 K intake temperature. As a result, it is found that this numerical investigation can contribute to the determination of proper fuel mixture and intake temperature for the problems such as extending the HCCI operation range, controlling the combustion, preventing knocking combustion and reduction of CO and HC emissions in HCCI combustion. Therefore, future work is recommended to improve the zero-dimensional model by combining it with conditional moment closure model and also experimental test rig develop for the HCCI engine.

PROBLEMS / CONSTRAINTS IF ANY *(Masalah/ Kekangan sekiranya ada)*

I	Not applicable

Date : *Tarikh*

Project Leader's Signature: *Tandatangan Ketua Projek*

COMMENTS, IF ANY/ ENDORSEMENT BY FACULTY (*Komen, sekiranya ada / Pengesahan oleh Fakulti)*	
J	**Recommend / Not Recommend / KIV / Need Ammendment** .... **Name:** *Nama:* **Signature:** *Tandatangan:* **Date:** *Tarikh:* **** Dean/TDR/Director/Deputy Director**
COMMENTS, IF ANY/ ENDORSEMENT BY RMC PNI (*Komen, sekiranya ada / Pengesahan oleh RMC PNI)*	
K	**Recommend / Not Recommend / KIV / Need Ammendment** .... **Name:** *Nama:* **Signature:** *Tandatangan:* **Date:** *Tarikh:*

LAMPIRAN B

PROFILE BOOK
INTERNAL GRANT: RDU1403126

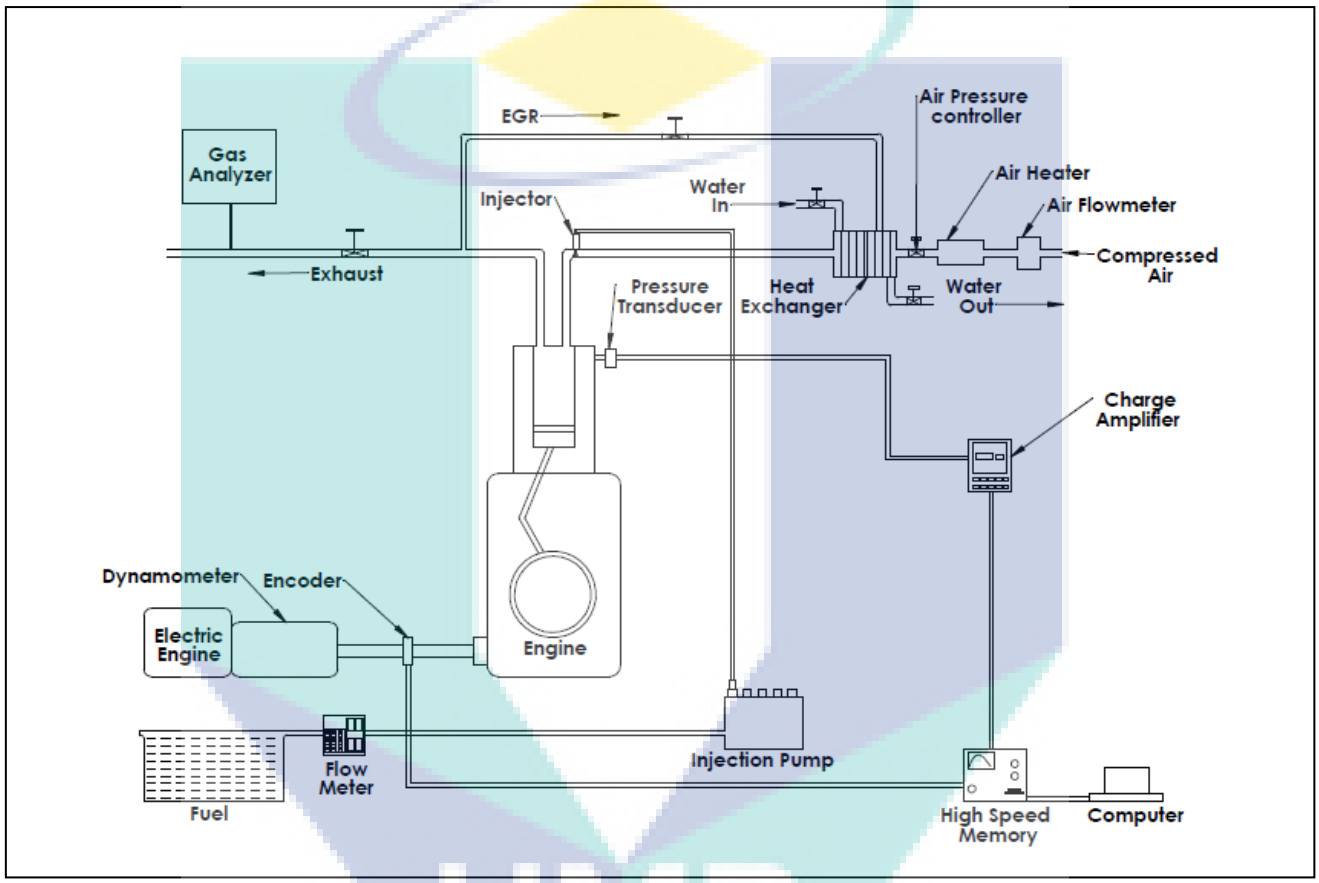

TITLE OF RESEARCH
IMPACT BIODIESEL FUEL CHARACTERISTICS ON ULTRA-LOW EMISSION HOMOGENEOUS CHARGE COMPRESSION IGNITION ENGINE

NAME OF PROJECT LEADER
PROFESSOR TS DR MD MUSTAFIZUR RAHMAN

NAME OF CO-RESEARCHERS
1. DR. MUHAMAD MAT NOOR, FTKMA
2. PM DR ABDUL ADAM ABDULLAH FTKMA
3. PROF. DATO DR ROSLI ABU BAKAR, FTKMA
4. PROF. DR. RIZALMAN MAMAT, FTKMA
5. PM DR KUMARAN KADIRGAMA, FTKMA
6. PM DR DEVARAJAN RAMASAMY, FTKMA

FACULTY OF MECHANICAL AND AUTOMOTIVE ENGINEERING TECHNOLOGY
E-mail: mustafizur@ump.edu.my
Field: AUTOMOTIVE ENGINEERING

ABSTRACT

Homogeneous charge compression ignition (HCCI) engine has been an active research area due to its potential for high fuel conversion efficiency and extremely low emissions of particulate matter and oxides of nitrogen (NO_x). However, the operational range using HCCI combustion in terms of speed and load is restricted because the start of combustion (SOC) and the heat release rate cannot be controlled directly. Depending only on the thermal history and chemical behavior of the cylinder contents, SOC is manipulated by precise manipulation of these variables through methods such as intake temperature and pressure conditioning, fuel blending, variable cylinder geometry, and variable valve timings. In order to design an engine for extended operational range as well as various fuels and blends of fuels, accurate models are needed which are able to model both combustion and performance. The objective of this study is to impact biodiesel fuel characteristics on ultra-low emission homogeneous charge compression ignition engine. In this study, a zero dimensional single-zone numerical simulation with reduced fuel chemistry of various fuels and blends of fuels was developed and validated. It is known for its advantage in reducing computational time compared with a multi-dimensional Computational Fluid Dynamics approach. The main focus of the study is to obtain an improved result for the zero-dimensional model, while the experimental results were used for the purpose of validation. The obtained results show good agreement with the experimental published results and capture important combustion phase trends as engine parameters are varied with a maximum percentage of error which is less than 6% for diesel HCCI and 4% for gasoline HCCI. The combustion phase advances and the combustion duration shorten with the increase of intake charge temperature and the decrease of the engine speed for both diesel and gasoline HCCI. The maximum load successfully increased with increasing the intake pressure. The highest load in this study was 11.27 bar in IMEPg at the condition of 200 kPa in intake air pressure and 333 K in intake air temperature for diesel HCCI and 10.86 bar in IMEPg at the condition of 200 kPa in intake air pressure and 393 K in intake air temperature for gasoline HCCI. It is found that the intake air pressure gives the most sensitive influence on HCCI combustion and performance characteristics. For various fuel blends, thermal efficiency was increased by about 17.71% with Bu30 compared to n-heptane at 393 K intake temperature. IMEP decreased at all intake temperatures with n-heptane. Very low amount of NO_x emissions were found with test fuels which is less than 2.5 ppm. NO_x emissions were increased with the increase of intake temperature. It is also seen that carbon monoxide (CO) emissions were increased with the increase of alcohol in the test fuels. Maximum CO emissions were found as 0.47% with E30 at 313 K intake temperature. Moreover, higher hydrocarbon (HC) emissions were obtained especially at lower intake temperature when ethanol was used as an additive fuel. Maximum HC emissions were found as 159.6 ppm with E30 test fuel at 313 K intake temperature. As a result, it is found that this numerical investigation can contribute to the determination of proper fuel mixture and intake temperature for the problems such as extending the HCCI operation range, controlling the combustion, preventing knocking combustion and reduction of CO and HC emissions in HCCI combustion. Therefore, future work is recommended to improve the zero-dimensional model by combining it with conditional moment closure model and also experimental test rig develop for the HCCI engine.

1. INTRODUCTION

1.1 Homogeneous Charge Compression Ignition

The concern about fuel economy and emissions is increasing day by day because these are the basic issues for internal combustion (IC) engine industry. The primary emissions from IC engines are nitrogen oxides (NO_x), particulate matter (PM), unburned hydrocarbon (HC) and carbon monoxide (CO). Temperature is the main factor for the formation of NO_x. In conventional compression ignition (CI) and spark ignition (SI) engines, high temperature is produced during combustion because of the stoichiometric air-fuel mixture. Thus, NO_x cannot be averted in conventional IC engines. The reason for the formation of PM is similar to NO_x. When the high temperature and rich mixture exist together in the combustion process, certainly PM produces. Especially, PM emissions cannot be averted at high load condition. The incomplete combustion is the main reason for the production of UHC and CO in IC engines. The thermal efficiency of conventional IC engines is very low which is another concern for the automotive industry. It has been seen from research that a higher compression ratio can provide higher thermal efficiency [1, 2]. Therefore, future combustion systems should incorporate high efficiency, high compression ratio engines. However, the compression ratio of SI engines cannot be increased so much because the high compression ratio creates abnormal combustion with a knock in SI engines [3].

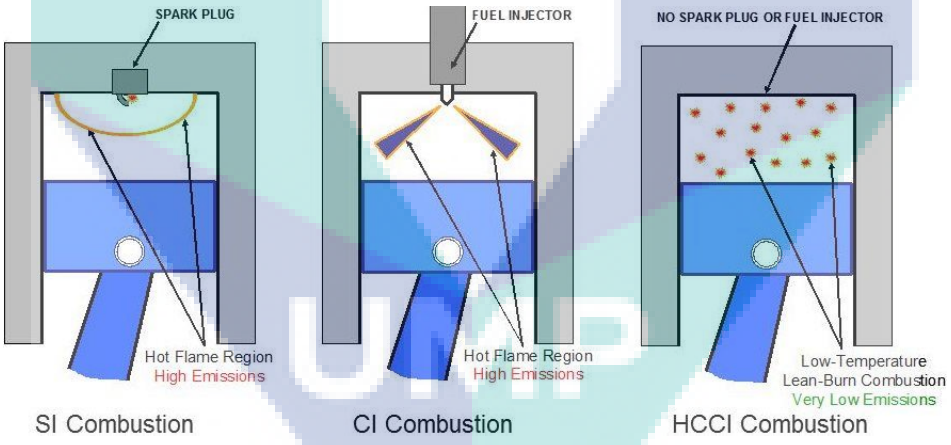

Figure 1.1 The differences between SI, CI, and HCCI engines, adapted from Lin, Hsu [4]

HCCI combustion is defined as a process by which a homogeneous mixture of air and fuel is compressed until auto-ignition occurs near the end of the compression stroke [5]. SI engines have a spark plug to initiate the combustion with a flame front propagating across the combustion chamber. CI engines have a fuel injector to inject the diesel and the combustion takes place in a compressed hot air region. HCCI engines have no spark plug or fuel injector and the combustion starts spontaneously in multiple locations. High engine efficiency can be achieved with low NO_x and PM emissions. Figure 1.1 shows the differences between SI, CI, and HCCI engines. HCCI combustion is noticeably faster than either compression ignition or spark ignition combustion [6]. HCCI combustion can improve the thermal efficiency and maintain low emissions as well as can be implemented by modifying either SI or CI engines [7]. A wide variety of fuels, a combination of fuels and alternative fuels can be used.

Usually, a lean air-fuel mixture is used in HCCI engines. It ignites automatically in several locations and is then burned volumetrically without visible flame propagation [8]. Once ignited combustion occurs very quickly and it is fully controlled by chemical kinetics rather than spark or ignition timing [9].

The advantages of HCCI technology are i) as HCCI engines are fuel-lean that can operate at diesel-like compression ratios (>15), thus achieving higher efficiencies than conventional SI gasoline engines [10]; ii) it can operate on a wide range of fuels [11]; iii) it can produce a cleaner combustion and lower emissions especially NO_x levels are almost negligible [12]. Alternatively, HCCI technology has some disadvantages such as high levels of UHC and CO as well as knocking under certain operating conditions [13]. In terms of emissions, diesel engines produce higher NO_x and PM or soot which require proper control strategies because of having negative health and environmental effect, which can be solved by using HCCI combustion engines [14]. As HCCI operates on lean mixtures, the peak temperatures are much lower than SI and CI. The low peak temperatures reduce the formation of NO_x. However, the low peak temperatures also lead to incomplete burning of fuel, especially near combustion chamber walls. This leads to high CO and HC emissions. An oxidizing catalyst can remove the regulated species because the exhaust is still oxygen-rich.

The HCCI diesel combustion is characterized by a set of several hundreds of species and complex reactions. This process consists of a two-stage heat release. The first stage of heat release occurs due to low-temperature reactions (LTR) and during this stage, a small portion of total energy (7–10%) is released, while the second stage of heat release occurs due to high temperature reactions [15]. During this stage, a huge amount of energy (approximately 90% of total energy) is released [16]. During LTR, fuel is consumed through an initial breakdown of HC fuel molecule which leads to form a hydrocarbon radical. This radical reacts with oxygen and form an alkylperoxy radical. The alkylperoxy radical is then changed into a hydroperoxy alkyl radical through an isomerization process. After that, a second oxygen molecule addition reaction occurs where an oxohydroperoxide radical is formed. This radical is further isomerized and decomposed into ketohydroperoxide species and OH radicals. A time delay exists between the LTR stage and the HTR stage which is known as the ‘‘negative temperature coefficient (NTC) regime” [17]. The alkylperoxy radicals decompose back into initial reactants, which help to form olefins and hydroperoxyl radicals. All the mentioned reactions are initiated at approximately 700 K and occur at modest reaction rates. Due to the heat release in this stage, the mixture temperature rises and when the temperature reaches at 900 K the HTR starts. In the HTR regime, mixture temperature rises rapidly and oxygen, as well as fuel molecules, are fully consumed to form carbon dioxide, water, carbon monoxide and hydrogen.

The formation of NO_x and soot plays a significant role to understand the fundamentals of HCCI combustion. The regions of the formation of NO_x and soot have been illustrated in Figure 1.2. The formation of NO_x is a complex process that involves the reactive combination of nitrogen found within the combustion air and organically bound nitrogen within the fuel itself. NO_x is a thermally produced gas and therefore its formation is largely dependent on the control of the combustion temperature [18]. It is seen that at low equivalence ratios and high flame temperatures usually, NO_x formation occurs. The formation of NO_x can be reduced by keeping the flame temperature below 2200 K [19]. On the other hand, soot formation occurs in regions of high equivalence ratios or fuel rich mixtures and moderate temperatures. Net soot emission is a balance between formation and oxidation can be reduced either increasing mixing or increasing oxidation [14]. In conventional diesel engines, a

representative fuel element would follow a path leading to both formations of both NO_x and soot emissions. Strategies to reduce NO_x formation during standard diesel operation normally lead to a penalty in soot emissions and vice versa.

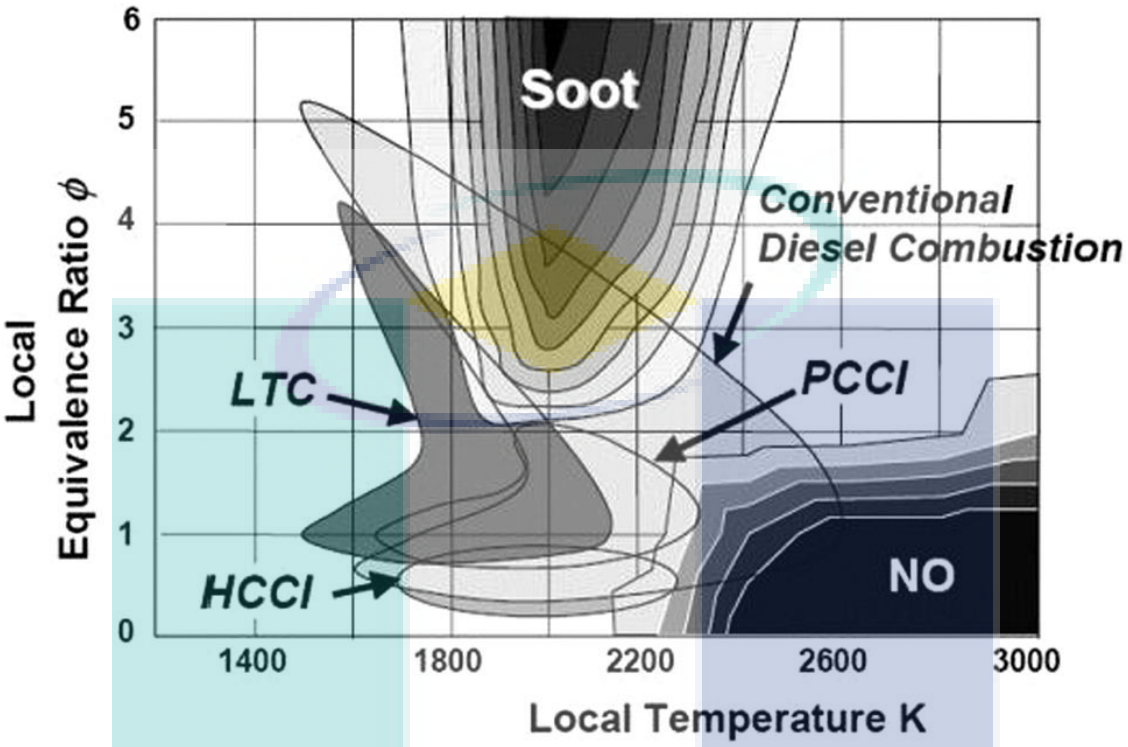

Figure 1.2. Equivalence ratios versus temperature (Soloiu, Duggan [20])

As both NO_x and soot emissions are strong functions of temperature and equivalence ratio, the most direct approach to reducing these emissions simultaneously is to carefully control the flame temperature and equivalence ratio [21]. In line with this approach, the main purposes of HCCI combustion are to concurrently lower the flame temperature and allow sufficient air and fuel mixing to increase the homogeneity of charge. From a conceptual point of view, when a thoroughly homogeneous in-cylinder mixture is formed, the pressure and temperature rise during the compression stroke resulted in simultaneous auto ignition across the whole cylinder. Local temperatures are maintained at low levels with the absence of a high-temperature flame front and NO_x formation is thus avoided [22]. Soot formation is also avoided due to the homogenized lean mixture which lowers local equivalence ratios [23]. The purpose of this study is to impact biodiesel fuel characteristics on ultra-low emission homogeneous charge compression ignition engine.

2. LITERATURE REVIEW

The effects of engine parameters and fuels and additives on HCCI engines and relevant numerical studies of HCCI engines was summarized in this section. There is a need to report the recent advancement of HCCI combustion due to the significance development of technology and which can be a replacement for conventional CI or SI engines. This chapter discusses the current issues for this technology where engine performance and emission characteristics of HCCI engines will be presented and compared with CI engines and SI engines. The performance of the HCCI engine is strongly dependent on the engine parameters and fuel type, and these affect the emission levels as well. Due to this, the effects of engine parameters as well as fuels and additives on HCCI engines will be described in the next section.

2.1 HCCI Diesel Combustion

The investigation on cylinder pressure in HCCI engines has been reported by many researchers [24-28]. Gajendra Singh et al. [24] investigated experimentally the combustion, performance and emission characteristics of HCCI engines using diesel and different percentages of biodiesel-diesel blend and compared the results with conventional diesel engines. The authors modified a double cylinder, four stroke and air cooled diesel engine for HCCI operation and used different percentages of EGR (0%, 15% and 30%). They reported that the cylinder pressure is higher in HCCI engines than conventional CI engines. However, by increasing the percentage of EGR, it can be lower and suitable for engine performance. Ganesh et al. [26] have also found similar results. Ramesh et al. [29] used hydrogen as a fuel to investigate the combustion characteristics of HCCI engines. They also observed the higher cylinder pressure and used CO_2 as an additive to keep the cylinder pressure at a reasonable level. Applying different techniques some researchers have found lower cylinder pressure in HCCI engines than CI engines. Lei Shi et al. [30] applied internal and external exhaust gas recirculation technique to reduce the cylinder pressure. Recirculation of cooled external exhaust gas was very helpful in this case. Francisco et al. [25] modified the cylinder used in their experiment to get a positive cylinder pressure. Turkcan et al. [28] also found similar results.

From the investigations done by many researchers on HCCI combustion mode, it can be reported that HRR of HCCI combustion is completely different from both CI and SI combustion [31]. Most of the researchers [25, 27, 28, 32, 33] found HRR is higher in HCCI engines than diesel engines. Jimenez et al. [25] investigated experimentally the combustion, performance and emission characteristics of HCCI engines using diesel and different percentages of the biodiesel-diesel blend as well as compared the results with conventional diesel engines. From the investigation, the authors reported that HRR is higher in HCCI engines than conventional CI engines. The imperfect air-fuel mixture was the reason for this occurrence. Swami Nathan et al. [33] and Gomes et al. [34] used different fuels i. e. acetylene and hydrogen to investigate the combustion characteristics of HCCI engines. In the case of HRR, they also found similar results like Jiménez-Espadafor, Torres [25]. Some researchers [24, 26, 35, 36] found opposite results i.e. lower HRR than diesel engines because of their initiatives. Ganesh et al. [26] modified a single cylinder, four stroke and direct injection diesel engine for HCCI operation. They also made a biodiesel vaporizer to vaporize the fuel perfectly so that it can mix with air to prepare a homogeneous

charge. Due to this reason, they observed lower HRR than diesel engines. Singh et al. [24] observed similar results while applying the same technique like Ganesh, Nagarajan [26] in a double cylinder, four strokes, air cooled and direct injection diesel engine. Zhang et al. [35] and Kulzer et al. [36] also found identical results in case of HRR. To reduce HRR in HCCI engines, the suitable mixture formation and appropriate auto-ignition chemistry play a vital role [37-39]. In addition, air-fuel equivalence ratio, engine speed and EGR have also effect on HRR in HCCI engines [31, 40]. Controlling this perfectly can provide a suitable HRR from HCCI engines. Most of the researchers [27, 33, 36, 41] observed that HCCI engines provide higher thermal efficiency than diesel engines. Swami et al. [41] have performed a study to measure the thermal efficiency of the HCCI engine and compare with conventional diesel engine while using biogas as fuel. The authors used different intake temperatures i. e. 80 ^{0}C, 100 ^{0}C and 135 ^{0}C. The main component of fuel was methane (>60%) and produced anaerobic fermentation of cellulose biomass materials [42]. It was reported that when the intake temperature was 135 ^{0}C, then thermal efficiency was higher than diesel engine. Gomes et al. [34] found that HCCI engines can provide 45% higher thermal efficiency than diesel engines when hydrogen is used as a fuel. Canakci [43] investigated combustion characteristics of HCCI engine using different boost pressures and gasoline as fuel. He also found similar results. Some of the researchers found opposite results i.e. lower thermal efficiency than conventional diesel engines due to inappropriate mixture, low fuel quality etc [24, 44-46]. Ganesh et al. in their two experiments [44, 45] found a negative results in case of thermal efficiency while investigating the combustion characteristics of HCCI engines in a single cylinder, four stroke, air cooled and direct injection diesel engine when used diesel as fuel. It was very difficult task to vaporize the diesel and mix it properly with air. Due to this reason, the mixture was not homogeneous and ultimately provided a lower thermal efficiency than diesel engine. However, same research team observed a higher thermal efficiency than diesel engine when biodiesel-diesel blend was used as a fuel [26]. They used a vaporizer to vaporize the fuel perfectly and were able to prepare a homogeneous mixture.

2.2 HCCI Gasoline Combustion

The in-cylinder pressure measurement is considered to be very important because it provides valuable information such as the peak pressure, P–V diagram indicated mean effective pressure, fuel supply effective pressure, heat release rate, combustion duration, ignition delay and so on [47]. It is the predominant view that HCCI engines provide higher cylinder pressure than SI engines [48-52]. Polovina et al. [48] investigated experimentally the combustion, performance and emission characteristics of HCCI engines using gasoline and different percentages of gasoline–ethanol blend, and compared with conventional SI and spark-assisted compression ignition engines under various conditions such as naturally aspirated, boosted, lean and stoichiometric. The authors modified a four-cylinder, four-stroke, naturally aspirated, air-cooled and port fuel-injected gasoline engine for HCCI combustion. The authors reported that at partial load, the cylinder pressure of HCCI is quite similar to that of conventional SI engines. However, at higher load the cylinder pressure exceeds the SI engine. Yap et al. [53] used hydrogen as a fuel to investigate the combustion and emission characteristics of HCCI engines. Their experiment was done in a modified single-cylinder, four-stroke and port fuel-injected gasoline engine and the authors also observed higher cylinder pressure than SI engines. The high cylinder pressure was at a reasonable level. Kobayashi et al. [54] investigated the combustion, performance and emission characteristics of HCCI engines. Their experiment was conducted on both single- and four-cylinder gasoline engines using gasoline as fuel. But they observed higher cylinder pressure. To mitigate it, they used a blend of

natural gas with gasoline. Milovanovic, Blundell [55] investigated the combustion characteristics of an HCCI engine in a modified gasoline engine under constant speed and different load. The authors concluded that by varying the amount of trapped residual gas in the fresh air/fuel mixture (inside the cylinder), the cylinder pressure can be controlled and hence also the auto-ignition timing and heat release rate.

Brake-specific fuel consumption (BSFC) is a measure of the fuel efficiency of any prime mover that burns fuel and produces rotational, or shaft, power [56]. It is typically used for comparing the efficiency of internal combustion engines with a shaft output [57]. The investigations on BSFC in HCCI engines have been reported by researchers [48, 49, 52, 58, 59]. Szybist et al. [49] modified a boosted single-cylinder research engine for HCCI combustion which was equipped with a direct injection fuelling system. Their purpose was to apply different control systems to achieve an HCCI high load limit. They found that to increase the load, it is also necessary to increase the manifold pressure and external EGR and that the BSFC was at a reasonable level at part load, but at high load operation, the difference with SI combustion becomes greater. Similarly, Yun et al. [58] investigated a spark-assisted HCCI combustion and double injection strategy to extend the higher operating load limit of an HCCI engine to maximize the fuel economy benefit of HCCI. The authors found that spark-assisted HCCI combustion was a key factor to reduce combustion noise and improve fuel economy at the high load condition. Alternatively, the double injection strategy could reduce combustion noise slightly, but the BSFC was increased due to incomplete combustion. Kobayashi et al. [54] and Al-khairi et al. [59] investigated the performance of an HCCI engine by modifying a gasoline engine and using natural gas as fuel. They found similar results in the case of the BSFC. Some of the researchers found the opposite results due to appropriate mixture homogeneity as well as complete combustion [52, 60, 61]. Hyvonen et al. [62] investigated the spark-assisted HCCI combustion in a five-cylinder variable compression ratio HCCI engine using gasoline. The authors found a lower BSFC than in the SI engine. Another experiment was done by Lemberger and Floweday [61] on a single-cylinder 25cc, air-cooled, 4-stroke spark ignition (SI) engine converted to run in HCCI mode with the aid of various combustion control systems and using diethyl ether as fuel. Later, the authors compared the performance result with an SI engine and found a lower BSFC than for SI.

The brake thermal efficiency (BTE) of an engine can be defined as the ratio of brake output power to input power and describes the brake power produced by an engine with respect to the energy supplied by the fuel. According to the review, most of the researchers observed that HCCI engines provide higher thermal efficiency than diesel engines [49-52, 63]. When an HCCI engine is modified from an SI engine it provides higher BTE than conventional SI engines. A study was performed by Gotoh et al. [51] to measure the BTE of an HCCI engine and compare the value with a conventional gasoline engine while using gasoline as fuel. They applied a blow-down supercharging system and varied the intake temperature and pressure. Ultimately, they came to the conclusion that by imposing the blow-down charging system the operating load limit of the HCCI engine can be increased along with the BTE. An investigation and comparison of combustion, performance and emission characteristics of two-stroke and four-stroke spark ignition and HCCI operations in a direct ignition gasoline engine were conducted by Zhang and Zhao [52]. They observed that, among all the experiments, when the engine was run in HCCI mode it provided the highest BTE. Similar experiments were done by Machrafi et al. [64] and He et al. [65], but the authors used different types of fuels, i.e. blends of iso-octane and n-heptane as well as gasoline and n-butanol. In all these cases the authors found higher BTE. Aceves et al. [66] proposed a multi-zone model for predicting the

combustion, performance and emissions characteristics of an HCCI combustion engine. From their prediction it was found that BTE was always higher than conventional SI engines in any load condition. Polovina et al. [48] investigated the combustion characteristics of an HCCI engine in a modified gasoline engine under various conditions, including naturally aspirated, boosted, lean and stoichiometric. The authors reported that at partial load, the BTE of HCCI is quite similar to that of conventional SI engines. However, at higher load, the BTE was less than for SI engines.

Table 2.1. Different experimental engine emissions results using various fuels in HCCI engines compared to CI engines

Engine	Test condition	Fuel	Emissions	Reference
1-cylinder, 4S, AC, CI, DI, CR: 17.5:1, RP: 4.4 kW, RS: 1500 rpm	Constant speed, different loads and different percentages of EGR (0% and 10%)	Diesel	↓: NOx, Smoke ↑: HC, CO	[45]
1-cylinder, 4S, CI, DI, CR: 15:1, RS: 1500 rpm	Constant speed and different loads	Diesel	↓: NOx, HC	[77]
1-cylinder, 4S, WC, NA, CI, CR: 14.8:1	Variable speed and different percentages of EGR (0%, 29%, 42% and 50%)	Diesel	↓: NOx, Smoke ↑: HC, CO	[30]
1-cylinder, 4S, CI, CR: 19:1, RP: 11 kW, RS: 3000 rpm	Variable speed and different loads	Diesel	↓: NOx, Smoke ↑: HC, CO	[78]
4-cylinder,High pressure common rail, CR: 18.5:1, RP: 87 kW, RS: 4000 rpm	Variable speed and different loads	Diesel	↓: NOx, soot	[79]
1-cylinder, 4S, NA, CI, DI, CR: 16.1:1, RP: 62 kW, RS: 1800 rpm	Variable speed and different loads	Gasoline	↓: NOx ↑: HC, CO	[43]
1-cylinder, 4S, NA, CI, DI, CR: 16.1:1, RP: 62 kW, RS: 1800 rpm	Variable speed and different loads	Gasoline	↓: NOx ↑: HC, CO	[27]
1-cylinder, 4S, WC, NA, CI, DI, CR: 17:1	Variable speed and different loads	Gasoline-Alcohol	↓: NOx ↑: HC, CO	[28]

2.3 Emissions Comparison

The United States, Europe, Japan and Singapore are imposing various standards on emissions from vehicles [67-69]. Emissions in HCCI engines consist of HC, CO, NO_x and PM. Various fuels used in HCCI engines have been proved to have low emissions levels of NO_x and PM [41] and high levels of UHC and CO [41, 70]. However, the emissions levels vary from one engine to another and are dependent on the operating conditions of the engine, fuel quality and the engine design [71]. This section presents a review of emission characteristics in terms of HC, CO and NO_x of HCCI engines using various fuels and illustrates an emission comparison among HCCI, CI and SI engines at Table 2.1-2.2. Carbon monoxide is mainly produced due to incomplete combustion of the fuel. Incomplete combustion occurs when flame

temperature cools down and progression to CO_2 remains incomplete [72]. It is reported that CO emission is higher in HCCI engines than diesel engines in the literature [24-28] and still a challenge for HCCI engines which should be solved very soon to get the full benefit from HCCI engines. Ganesh et al. [26] reported that CO is higher in HCCI engines due to the nature of this type of combustion. The authors used different fuels but observed the similar results in case of CO emission. The amount of CO_2 and CO are dependent on the combustion efficiency, where the combustion efficiency can be defined as the ratio of CO_2 to the total of fuel carbon present in the exhaust including CO, CO_2 and UHC [73]. CO is formed by following RH-R-RO_2-RCHO-RCO-CO equation, where R is the hydrocarbon radical [74]. CO is mainly formed in the crevices of the cylinder which are so cold for complete combustion [75]. That's why this problem needs to be solved for producing lower CO emission. In addition, for the complete reaction of the conversion from CO to CO_2 needs temperature above 1500 K [76]. However, CO formation occurs in case of HCCI combustion at low load peak burned gas temperature remains below that required level.

Table 2.2. Different experimental engine emissions results using various fuels in HCCI engines compared to SI engine

Engine	Test condition	Fuel	Emissions	Reference
1-cylinder, 4S, AC, GDI, CR: 11.3:1, RS: 2500 rpm	Variable speed and fixed load	Gasoline	↑: HC, CO ↓: NO_x, PM	[80]
1-cylinder, 4S, AC, PFI, CR: 12:1, RS: 1500 rpm	Constant speed, different loads and different percentages of EGR	Gasoline	↓: NO_x	[18]
1-cylinder, 4S, AC, GDI, CR: 11.78:1, RS: 1500 rpm	Constant speed, different loads and different percentages of EGR	Gasoline	↑: HC, CO ↓: NO_x	[52]
1-cylinder, 4S, WC, PFI, CR: 10.5:1, RS: 2000 rpm	Constant speed and different loads	Gasoline	↓: HC, CO, NO_x	[55]
5-cylinder, 4S, AC, PFI, CR: 10-30:1	Constant speed and different loads	Gasoline	↑: HC, CO ↓: NO_x	[62]
1-cylinder, 4S, AC, GDI, CR: 11.85:1, RS: 2000 rpm	Constant speed and different loads	Gasoline-ethanol blend	↑: NO_x	[81]
1-cylinder, 4S, AC, PFI, CR: 14:1, RS: 2100 rpm	Constant speed and different loads	Gasoline and CNG	↑: CO ↓: HC, NO_x	[59]
1-cylinder, 4S, AC, PFI, CR: 10.66:1, RS: 1500 rpm	Variable speed and fixed load	Gasoline and n-butanol	↓: NO_x	[65]
1-cylinder, 4S, AC, PFI, CR: 10.66:1, RS: 1500 rpm	Variable speed and fixed load	n-butanol	↓: NO_x	[63]
1-cylinder, 4S, AC, PFI, CR: 12.5:1 &15:1, RS: 1500 rpm	Constant speed and variable compression ratio	Propane	↑: HC, CO ↓: NO_x	[53]

Hydrocarbons in the exhaust exist for one of two reasons either from the fuel that avoids combustion or from intermediate species of hydrocarbons that are formed during combustion and not completely combusted. The formation of hydrocarbons is typically due to local flame extinction, either by misfire or gaps in the cylinder geometry [12]. Hydrocarbons in the exhaust exist for one of two reasons either from the fuel that avoids combustion or from intermediate species of hydrocarbons that are

formed during combustion and not completely combusted. The formation of hydrocarbons is typically due to local flame extinction, either by misfire or gaps in the cylinder geometry [12]. It is a predominant viewpoint that HC emissions increases when HCCI combustion is applied [24-28] and like CO emission, it is another challenge of HCCI engines. Ganesh et al. [44] reported that HC is higher in HCCI engines due to the nature of this type of combustion. The authors used different fuels but observed the similar results in case of HC emission. For low combustion temperature, incomplete combustion occurs and ultimately HC emissions is produced [45, 82]. HC is mainly formed in the crevices of the cylinder which are so cold for complete consumption [75]. Higher concentrations of hydrogen and natural gas in diesel engines have the ability to reduce UHC and CO emission levels because the gaseous state of hydrogen and natural gas will reduce the wall wetting effect on the cylinder liner [83]. Since HCCI engines typically operate fuel lean, the final flame temperature is usually well below 2000 K [14]. At this low post-combustion temperature chemical reactions that produce NO_x are essentially inactive [84].

NO_x is generally formed in a high temperature reaction, where the nitrogen in air dissociates into nitrogen radicals to form NO when reacting with oxygen. NO is converted to NO_2 when further reactions occur in the chamber. From the review, it is the common conclusion that NO_x emission is negligible in HCCI engines compared to CI engines [24, 26-28, 32]. Gajendra Singh et al. [24] investigated experimentally the combustion, performance and emission characteristics of HCCI engines using diesel and different percentages of the biodiesel-diesel blend as well as compared the results with conventional diesel engines. The authors modified a double cylinder, four stroke and air cooled diesel engine for HCCI operation and used different percentages of EGR (0%, 15% and 30%). From the investigation, the authors reported that NO_x emission is very low in HCCI engines compared to conventional CI engines. NO_x formation is dependent on equivalence ratio. Tanaka et al. [85] found that the equivalence ratio of more than 0.33 is the possible reason for a substantial increase in NO_x. Authors in literature [21, 86] used high compression ratio engines in their experiment and observed a very low amount of NO_x. NO_x emission can also be reduced by applying EGR technique which was proved by Bression, Soleri [82].

2.4 HCCI Gasoline Combustion

It is reported that CO emission is higher in HCCI engines than gasoline engines [52, 54, 59, 80]. Kobayashi et al. [54] investigated the combustion, performance and emission characteristics of HCCI engines. Their experiment was conducted on both single-and four-cylinder gasoline engines using gasoline as fuel. However, they observed higher CO than in SI engines. Aceves et al. [66] proposed a multi-zone model for predicting the combustion, performance and emissions characteristics of an HCCI combustion engine. From their prediction it was found that CO was always higher than in conventional SI engines in any load condition. It is the predominant viewpoint that HC emissions increase when HCCI combustion is applied [54, 61, 62] and, like CO emission, this is another challenge with HCCI engines. Kobayashi et al. [54] investigated the emissions characteristics of an HCCI engine by modifying a gasoline engine and using natural gas as fuel. They found higher HC than in SI engines. A similar experiment was done by Lemberger and Floweday [61] on a single-cylinder 25cc, air-cooled, 4-stroke SI engine converted to run in HCCI mode with the aid of various combustion control systems and using diethyl ether (DEE) as fuel. Later they compared the emission result with an SI engine and found higher HC than for SI. NO_x emission is negligible in HCCI engines compared to SI engines [48, 49, 52, 63, 65]. Polovina et al. [48] [48][48][48][48][48][48][48][48] investigated experimentally the combustion, performance and emission characteristics of HCCI

engines using gasoline and different percentages of gasoline–ethanol blend as well as comparing with conventional SI and spark-assisted compression ignition engines under various conditions including naturally aspirated, boosted, lean and stoichiometric. The authors modified a four-cylinder, four-stroke, naturally aspirated, air-cooled and port fuel-injected gasoline engine for HCCI combustion. The authors reported that NO_x emission is very low for every load condition. Kobayashi et al. [54] investigated the combustion, performance and emission characteristics of HCCI engines. Their experiment was conducted on both single- and four- cylinder gasoline engines by using gasoline. The authors also observed lower NO_x than in SI engines. Similarly, Lemberger and Floweday [61] modified a single-cylinder 25cc, air-cooled, 4-stroke spark ignition (SI) engine for HCCI combustion. Their observations were also similar to those of others. Aceves et al. [66] proposed a multi-zone model for predicting the combustion, performance and emissions characteristics of an HCCI combustion engine. From their prediction, it was found that NO_x was always lower than conventional SI engines in any load condition.

2.5 Effects of Engine Parameters

In order to develop an appreciable control method to optimize ignition timing and smooth heat release rate, it is very important to understand the effects of engine parameters on the ignition timing, combustion rate, performance and emissions [87]. This section presents a review of the effects of different engine parameters such as intake temperature, intake pressure and compression ratio on HCCI engines using various fuels, with some brief discussion.

2.5.1 Intake Temperature

One of the main parameters to control HCCI combustion is the intake air temperature, which affects the time–temperature history of the mixture. High intake temperature advances the start of combustion but causes a reduction in the volumetric efficiency [88]. Intake charge temperature affects the combustion and formation of emissions through two distinct pathways. When temperature is lowered, ignition delay is extended leading to enhanced air/fuel premixing. Additionally, the adiabatic flame temperature of a fuel parcel is decreased when it is mixed to a particular equivalence ratio. This means that fuel element is steered away from the NO_x–soot formation region on the equivalence ratios–temperature map. Lu, Chen [87] found that the intake temperature plays the most sensitive influence on the HCCI combustion characteristics. They showed that the combustion phase was advanced, and the combustion duration was shortened with the increase of intake charge temperature. They also showed that increasing intake charge temperature from 31^{o}C to 54^{o}C increased NO_x emissions linearly from approximately 10 ppm to 50 ppm when n-heptane fuel was combusted at fixed fuel delivery rate, engine speed and 30% EGR. This is in agreement with another HCCI work whereby NO_x increased when inlet air temperature increased from 35^{o}C to 80^{o}C [89]. Both unburned HC and CO were observed to be unaffected by intake temperature [87]. Experiments conducted on an HSDI diesel engine revealed that peak soot luminosity was markedly reduced when intake temperature decreased from 110^{o}C to 30^{o}C under a load condition of 3 bar IMEP [90]. This was attributed to both lower soot temperatures and reduced soot formation. Nonetheless, in-cylinder soot luminosity was clearly observed even at 30^{o}C which indicated that complete eradication of soot formation was difficult with typical fuel injection system parameters.

2.5.2 Intake Pressure

Turbocharging is used in HCCI operation to extend the operating load range [91-93]. This is particularly relevant in HCCI operations whereby reasonably high EGR rates are typically employed to control combustion and limit NO_x formation. The resulting dilution limits the amount of fuel that can be added for a fixed charge mass leading to a loss in engine power. To counter this for given engine size, more mass needs to be forced through the engine through turbocharging. By supercharging to 86 kPa and increasing the fuel quantity at a lowered compression ratio of 12.5, the power output could be increased to nearly the full load of conventional, naturally aspirated diesel combustion. Similarly, in the premixed compression ignition combustion system, a boost pressure of 80 kPa produced an output which was comparable to that of the full load of conventional, naturally aspirated diesel combustion [94]. Tests with n-heptane in a Cooperative Fuels Research engine operated in HCCI mode showed that raising the intake pressure from approximately 117.5 kPa to 152.5 kPa resulted in a directly proportional increase in IMEP when all influential parameters such as compression ratio, intake charge temperature, EGR rate and equivalence ratio were kept constant [95]. In another study, turbocharging on a six-cylinder diesel engine achieved high loads of up to 16 bar BMEP with ultra-low specific NO_x emissions (0.1 g/kW-hr) [96]. This compares to 21 bar BMEP for the same engine under standard diesel operation. Evaluation of boosting strategies for HCCI applications have been carried out by Olsson, Tunestål [97]. The dilution required to limit NO_x necessitates the use of much more boost compared to conventional engines for the same load. When high boost is required, turbocharger efficiency was presented to be very important for HCCI in order to reduce pumping losses. For high load applications, two stages turbocharging with inter-cooling is recommended. Better control of the turbocharger such as using variable geometry turbocharger avoids unnecessary pumping work through 'over boost'.

2.5.3 Compression Ratio

By lowering the compression ratio, the ignition delay is prolonged which allows complete injection of all fuels prior to ignition, a prerequisite for premixed combustion and a reduction in the gas temperature of the combustion field at TDC of the compression stroke [14]. Reducing compression ratio from 18:1 to 16:1 was part of the strategy used in the second generation of modulated kinetics diesel engines to extend low temperature, premixed combustion to higher load conditions [98]. It has been demonstrated by Olsson, Tunestål [2] that knock in HCCI diesel combustion can be prevented by reducing the compression ratio. When compression ratio is reduced, the accompanying reduction in temperature rise of the end gas prevents explosive self-ignition from occurring. Peng, Zhao [99] conducted experiments on a four-stroke, single cylinder, variable compression ratio engine using n-heptane which verified the effects of compression ratio on HCCI combustion. The results showed that the possibility of knocking decreased, with the knock limit pulled to lower air fuel ratio region (richer mixture) when compression ratio was reduced from 18:1 to 12:1. The maximum IMEP attainable on this engine thus increased from 2.7 bar to 3.5 bar. Experiments carried out on a PCCI engine demonstrated that under premixed combustion, NO_x emissions were only mildly reduced when compression ratio was reduced from 18.4:1 to 16.0:1 within the SOI timing range of 5°BTDC to 3°ATDC [100]. Soot emissions, unlike NO_x, were reduced more markedly when compression ratio reduced. The retardation can explain the reductions in NOx and soot emissions in ignition delay which leads to a reduction in the gas temperature at TDC of the compression stroke and more complete mixing of air and fuel mixture.

3 METHODOLOGY

3.1 NUMERICAL MODELING

Modeling combustion engines using computer codes is an important investigative technique. There are a number of different factors to be considered when developing a numerical model - chemistry, heat transfer, mechanical behavior, and fluid dynamics to name a few. In this study, a zero-dimensional single zone model for HCCI engine was established using MATLAB. The model is called the zero-dimensional model because time is the only independent variable used in this model. The proposed method takes into account the detailed thermodynamic aspects of engine. The model integrates the ordinary differential equation system corresponding to the chemical and thermal evolution of a closed homogeneous system under an imposed volume history reproducing the engine cycle. This single-zone in time model treats the cylindrical combustion chamber as a uniform reactor with uniform temperature, pressure, and composition throughout. The reactor volume changes based on slider-crank relations that determine the motion of the piston in the engine cylinder. This kind of model aims to simulate the auto-ignition process in the core of the air-fuel mixture and enables the use of detailed chemical kinetic models with which we can investigate the chemical reactions contributing to cylinder inside pressure and temperature. The accumulated gas is assumed to be ideal gas. The models used two different types of chemical reaction mechanisms to model the fuels because two types of engine configurations were used. This is to ensure that the model works in both engine conditions. This Chapter will describe chemical kinetics mechanisms for diesel, gasoline and other test fuels first as well as emissions formation. Then the equations used in zero-dimensional single zone modeling will be presented in detail. To understand how the numerical code works an algorithm flow chart will be presented. Combustion and performance parameters will be described in brief. At the end of the Chapter chemical properties of the test fuels will be presented.

3.1.1 Chemical Kinetics Mechanisms

A combustion event involves an extraordinary amount of elementary chemical reactions. Each reaction has a designated pre-exponential term (A, $l/cm^3mol^{-1}sec^{-1}$), temperature dependent exponent (*b*, no units), and activation energy (E_A, in kJ/mol) which are used to describe the reaction rate coefficient (k) according to Eq. (3.1).

$$k = AT^b \exp\left(\frac{-E_A}{RT}\right) \tag{3.1}$$

The development of chemical mechanisms for numerical modeling is an ongoing research. The researchers are testing, refining, and updating the values. Validation through comparisons with experimental results from shock tube and rapid compression machine experiments is one of the appropriate approaches. These mechanisms which can include on the order of 1000's of species (in the case of diesel fuel, for example) can quickly become cumbersome when running complex models. Therefore, another approach in the development of chemical mechanisms focuses on coming up with smaller mechanisms which still provide a desired degree of accuracy. This is done by constraining the conditions considered in the validation steps so that certain intermediate species and reactions can be ignored. These smaller mechanisms are often called skeletal or reduced mechanisms, with reduced mechanisms being the most drastically constrained and application-specific.

3.1.2 Diesel Mechanism

A chemical reaction mechanism is used to solve the chemical reactions during combustion. For diesel fuelled HCCI engines, a reduced diesel fuel surrogate mechanism [101] was used to simulate the diesel combustion. Pei and his co-workers assembled a kinetic mechanism describing the oxidation of n-dodecane/m-xylene mixture based on recently published kinetic mechanisms developed by the Lawrence Livermore National Laboratory. The detailed multi-component mechanism for n-dodecane and m-xylene was developed by combining the previously developed n-dodecane mechanism [102] with a recently developed mechanism detailing the combustion of the xylene isomers [101]. The two parent mechanisms were individually validated against an extensive set of experimental data for both fuels, including ignition delay time, speciation and laminar flame speed data. The detailed mechanisms, containing 2885 species and 11754 reactions, has been reduced using a combination of directed relation graph with expert knowledge [103] and directed relation graph aided sensitivity analysis algorithms coupled with isomer lumping. The resulting mechanism, including 163 species and 887 reactions, has been successfully applied to the simulation of 3D diesel-like spray combustion using a commercially available CFD code. This reduced mechanism for diesel surrogate was used in this study.

3.1.3 Gasoline Mechanism

In this study a 4-component surrogate was used to model gasoline fuel. This surrogate was developed by Mehl, Chen [104] at Lawrence Livermore National Laboratory. The surrogate is comprised of isooctane, *n*-heptane, toluene and 2-pentene, and the relative proportion of each component by mass fraction is given in Table 3.1.

Table 3.1 Gasoline surrogate composition

Component	Mass fraction
iso-octane	0.5413
n-heptane	0.1488
Toluene	0.2738
2-pentene	0.0361

In order to determine the composition of the surrogate, Mehl and coworkers used both composition of real gasoline (in terms of aromatics, olefins, alkanes and average molecular weight) as well as reactivity of gasoline (autoignition properties) to formulate a surrogate having a similar overall representation of various kinds of hydrocarbons and having similar (RON + MON)/2 as gasoline where RON stands for Research Octane Number and MON stands for Motor Octane Number. The choice of isooctane, *n*-heptane and toluene has been attributed to historical reasons, since they fit well within the molecular weight range of interest, and have been traditionally well understood within the combustion community. The addition of 2-pentene to represent olefins has been attributed to this molecule matching the typical molecular weight of olefins found in gasoline, and also because it has the highest octane number and sensitivity. A detailed chemical kinetic mechanism for this surrogate was developed by Mehl, Pitz [105], which consists of roughly 1400 species and 5000 reactions. This

mechanism was validated against gasoline shock tube data over a range of temperatures and pressures. However, it is computationally infeasible to incorporate such a large mechanism within a 3-D CFD simulation; hence the same group [104] also developed a reduced 312-species, 1488-reaction chemical kinetic mechanism based on the detailed mechanism, intended for 3-D CFD simulation of HCCI engines. This model was validated against HCCI engine experiments by Mehl, Pitz [106] over a range of intake pressure and load conditions, and was found to capture features such as intermediate temperature heat release [107] which are thought to be unique to gasoline fuel chemistry at higher pressures near TDC. This 312-species mechanism along with the 4-component gasoline surrogate was used in this study.

3.2 Mechanisms for Different Fuels and Blends of Fuels

A reduced *n*-heptane mechanism [108] was used to simulate *n*-heptane fuel in the HCCI combustion. The mechanism consists of 159 species and 770 elementary reactions. For *n*-heptane/ethanol blend fuel a reduced ethanol mechanism was combined with the *n*-heptane mechanism [109]. The final mechanism consists of 167 species and 1591 elementary reactions. In addition, for *n*-heptane/butanol blend fuel a reduced *n*-butanol mechanism was combined with the *n*-heptane mechanism [110]. The final mechanism consists of 181 species and 1703 elementary reactions.

3.2.1 Mechanism of Emissions Formation

Exhaust emissions consist mainly of direct combustion products, such as water and carbon dioxide, and pollutants such as CO, UHC and NO_x (which refers to the combination of NO and NO_2). The CO and UHC pollutants are a consequence of incomplete combustion. With rich air-fuel mixtures there is not enough oxygen to ensure oxidation of the carbon in the fuel to CO_2, also the carbon monoxide oxidation also freeze with the drop in temperature during the expansion stroke. To improve drivability during cold starts, the fuel flow is increased to compensate for slow fuel vaporization. However, this strategy leads to an increase in CO emissions as well as UHC. The CO formation can be summarized in the following reaction,

$$RH \rightarrow R \rightarrow RO2 \rightarrow RCHO \rightarrow RCO \rightarrow CO$$

where R is the hydrocarbon radical. The carbon monoxide formed is then oxidized to carbon dioxide at a slower rate via the principal oxidation reaction,

$$CO + OH \longleftrightarrow CO2 + H$$

There are several ways leading into the formation of unburned hydrocarbons. Due to the increasing cylinder pressure forces during the compression stroke part of the air-fuel mixture is trapped into the crevices, this mixture will not be exposed to the high temperatures and it will remain unburned. These unburned gases will then leave the crevices during exhaust stroke. Other sources of formation of UHC are the cold cylinder walls that lead to flame termination before the completion of the oxidation reactions. Engine oil left in thin films on the cylinder wall and piston can absorb and desorbs hydrocarbons before and after combustion, contributing as well to the formation of UHC.

The formation of NO_x is a complex process that involves the reactive combination of nitrogen found within the combustion air and organically bound nitrogen within the fuel itself. NO_x is a thermally produced gas and therefore its formation is largely dependent on the control of the combustion temperature. There

are many other mechanisms from which NO_x can be produced, but thermal and prompt NO are more relevant in the internal combustion engines application [21, 111-113].

In the combustion of clean fuels (fuels not containing nitrogen compounds), oxidation of atmospheric nitrogen by the thermal mechanism is a major source of NO_x emissions. The three principal reactions that comprise the thermal NO formation mechanism are,

$$O + N2 \longleftrightarrow NO + N$$

$$N + O2 \longleftrightarrow NO + O$$

$$N + OH \longleftrightarrow NO + H$$

The first two reactions compose a chain sequence in which a small amount of atomic oxygen can produce large amounts of NO. This mechanism, often called the Zeldovich mechanism, is very sensitive to temperature not only because the high activation energy of the first reaction, but also because the concentration of oxygen atoms in flames increases rapidly with increasing temperature [21, 111-113].

Nitric oxide formation rates in combustion of hydrocarbon fuels can exceed those attributable to the thermal mechanism discussed above, especially for fuel-rich conditions. This rapidly formed NO was termed prompt NO, since it's rapid and is confined to regions near the flame zone.

$$CH + N2 \longleftrightarrow HCN + N$$

$$CH2 + N2 \longleftrightarrow HCN + NH$$

$$CH2 + N2 \longleftrightarrow H2CN + N$$

$$C + N2 \longleftrightarrow CN + N$$
$$N + O2 \rightarrow NO + O$$

$$N + OH \rightarrow NO + H$$

It has been shown that, prompt NO in hydrocarbon flames is formed primarily by a reaction sequence of hydrocarbon radicals with molecular nitrogen, leading to formation of amines or cyano compounds that subsequently react to form NO. Numerous studies showed that CH and CH_2 are the hydrocarbon radicals that most contribute to the formation of prompt NO [21, 111-113].

In HCCI, combustion occurs through chemical oxidation, thus, the reached maximum temperature is determined by the energy content of the fuel/air/residuals mixture, giving lower maximum temperatures than comparable with SI or CI. While the Zeldovich mechanism (thermal NO) is adequate for calculating NO_x emissions in SI or CI engines, it is safe to say that it doesn't accurately predict these emissions on HCCI combustion. Studies on lean combustors showed that NO_x is largely formed through N_2O paths. It appears believable that N_2O reaction pathways would play an important role in NO_x formation also for HCCI engines [21, 111-113]. To predict the NO_x formation accurately, a NO_x mechanism prepared by Miller and Bowman [21] was integrated with all the mechanisms. For this reason, 7 extra species were added. The species are NO, NO_2, NO_3, N_2O, HONO, HNO, and CH_3O_2. Ultimately, 27

reactions were added with all the mechanisms. The reaction rates for all the reactions were taken from Miller and Bowman [21] and Mueller, Yetter [114]. For completeness, the added NO_x mechanism reaction rates are summarized in Table 3.2.

Table 3.2 NO_x kinetic mechanism reaction rates parameters for *A*, *b*, and E_A

S/L	Reaction (cm^3 – mol – sec – cal - k)	*A*	*b*	E_A
1	NO+O(+M)=NO2(+M)	3.00E+13	0.00	0.0E+00
2	NO+H(+M)=HNO(+M)	1.52E+15	-0.41	0.0E+00
3	NO+OH(+M)=HONO(+M)	1.10E+14	-0.30	0.0E+00
4	NO2+H2=HONO+H	0.733E+12	0.0E+0	2.881E+04
5	NO2+O=O2+NO	1.05E+14	-0.52	0.0E+00
6	NO2+O(+M)=NO3(+M)	1.33E+13	0.00	0.0E+00
7	NO2+H=NO+OH	1.32E+14	0.00	3.62E+02
8	HO2+NO=NO2+OH	2.11E+12	0.00	-4.790E+02
9	NO2+NO2=NO3+NO	9.64E+09	0.73	2.092E+04
10	NO2+NO2=2NO+O2	1.63E+12	0.00	2.612E+04
11	HNO+H=NO+H2	4.4E+11	0.72	650.0
12	HNO+O=OH+NO	1.81E+13	0.00	0.0E+00
13	HNO+OH=H2O+NO	1.30E+7	1.88	-956.0
14	HNO+NO=N2O+OH	2.00E+12	0.00	26000.0
15	HNO+NO2=HONO+NO	6.02E+11	0.00	1.987E+03
16	HNO+HNO=H2O+N2O	8.51E+08	0.00	3.080E+03
17	HONO+O=OH+NO2	1.20E+13	0.00	5.961E+03
18	HONO+OH=H2O+NO2	1.7E+12	0.00	-5.200E+02
19	N2O(+M)=N2+O(+M)	7.91E+10	0.00	56,024
20	N2O+O=O2+N2	1.00E+14	0.00	2.80E+04
21	N2O+O=NO+NO	1.00E+14	0.00	2.80E+04
22	N2O+H=N2+OH (DUP)	2.53E+10	0.00	4.550E+03
23	N2O+H=N2+OH (DUP)	2.23E+14	0.00	1.675E+04
24	N2O+OH=HO2+N2	2.0E+12	0.00	40000.0
25	NO+N2O=NO2+N2	1.0E+14	0.00	50000.0
26	CH3O2+NO=CH3O+NO2	2.530E+12	0.00	-358.00
27	CH3+O2(+M)=CH3O2(+M)	1.006E+08	1.630	0.00

3.3 Numerical Solutions

A zero-dimensional model solves the first law of thermodynamics equations, as presented in Eq. (3.31). The numerical solution for the temperature change is straightforward because the equation is in the form of a first-order ordinary differential equation. The equation was rearranged so that the change in temperature is on the left hand side. Then, a stiff solver was used to solve Eqs. (3.28) and (3.31) simultaneously. A flow chart of the model is presented in Figure 3.1. The model was coded so that the simulation runs based on the value of crank angle (CA), instead of the pre-defined process with pre-defined combustion, as done by Shaver, Gerdes [115], Canova, Garcin [116] and Killingsworth, Aceves [10]. A pre-defined or segregated process is where the simulation code is divided according to the engine cycle: intake, compression, power and exhaust. Each cycle uses a different set of equations to obtain temperature or pressure change across the CA, which is based on the ideal gas law equation. Then, the ignition occurs based on the pre-defined ignition location with estimated combustion duration, where the ignition delay has been measured according to the experiment. There is no detailed chemical reaction involved. For the simulation based on the value of CA, it uses the energy equation for the entire engine cycle to solve the temperature change in the chamber with detailed

chemical reactions involved. This method gives an advantage in predicting the chemical reaction behavior along the CA step, because the chemical reactions fully control the HCCI engines.

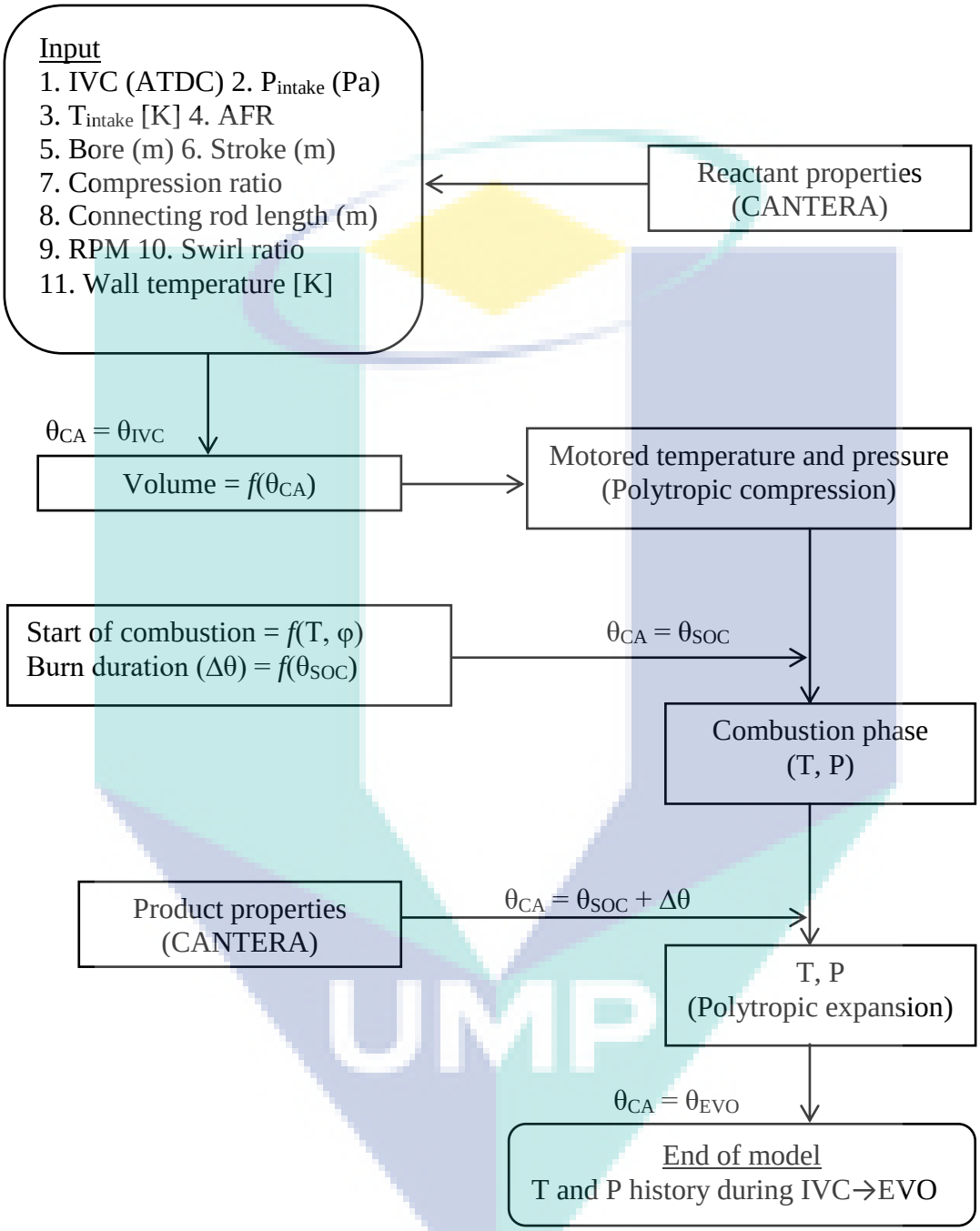

Figure 3.1 An algorithm flow chart for zero-dimensional single-zone model simulation

At the beginning of the simulation, the engine parameters and initial operating condition were defined, which were based on the experimental data [51, 117]. Then, the mixture composition in the combustion chamber and inlet manifold was initialized. It was assumed that the initial composition in the combustion chamber before IVO consists of only air and a mixture of air and fuel is introduced after the IVO. A typical valve profile was determined based on Eq. (3.18), which was used to represent the valve motion and also to get the inlet mass flow rate ($\dot{m}_{in}$). The simulation began from 0°CA, where the piston was at TDC, and finished at EVO. The

entire simulation consists of three parts: before IVO, before IVC and before EVO, as shown in Figure 3.1. For the first part, the piston was in a downward motion and the air was expanded before being mixed with the intake mixture. Once the intake valve was opened (second part), the air in the combustion chamber was mixed with the intake mixture. In this process, the mass was added to the combustion chamber based on Eq. (3.27). The cylinder volume was expanding and it is expected that the mixture temperature was decreasing at this stage. The final part is where the main combustion occurred, which was after IVC and before EVO. At this stage, the piston was in upward motion after IVC, compressing the gas mixture. The chemical kinetics plays an important role as it determines the start of combustion. Once the piston passes the TDC mark, it is in downward motion again, expanding the mixture and the simulation stops at EVO. The simulation solves the energy and species equations for the entire process. Therefore, this technique has eliminated the segregated process as usually done in zero-dimensional modeling. Segregated process is where the simulation is divided into four parts in one engine cycle: intake, compression, expansion and exhaust. Thus, the simulation uses four different sets of equations to cater for each process. In this study, the simulation uses only one set of equations for all the processes. This ensures the in-cylinder properties are consistent from one process to another. Cantera is an open source software package for chemical kinetics mechanism and is widely used [118]. New researchers could easily adopt Cantera for their research needs given the software's capability to integrate with MATLAB, FORTRAN and Python languages. The chemical kinetics mechanism files can be obtained in Chemkin format, where the file is then be converted to a Cantera-readable file. The use of a chemical reaction mechanism enables the study of the chemical species interaction, where the interaction is influenced by the temperature, pressure and species mass fraction. Furthermore, the chemical reaction mechanism would be able to give a better understanding in the combustion study. The base code used in this study for zero-dimensional single zone engine model written in MATLAB and using Cantera for the chemical kinetics calculations is included.

3.4 Combustion Parameters

The heat release profiles obtained from the in-cylinder pressure traces can be used to develop a characterization of the start of combustion (SOC). The HCCI combustion is considered to start as the crank angle at 10% of the cumulative heat release occurs. A graphical representation of this metric is shown in Figure 3.7 [119]. The combustion duration is often defined as the time between 10% and 90% cumulative heat releases. This is often referred to as CA10-90. The heat release duration is a good measure of the combustion event's time interval. A typical HCCI engine experiences an extremely rapid pressure event and thus short combustion duration. Therefore, an elongated heat release profile is desirable as it shows a less violent (smaller pressure rise rate) event. A graphical representation of this metric is shown in Figure 3.7.

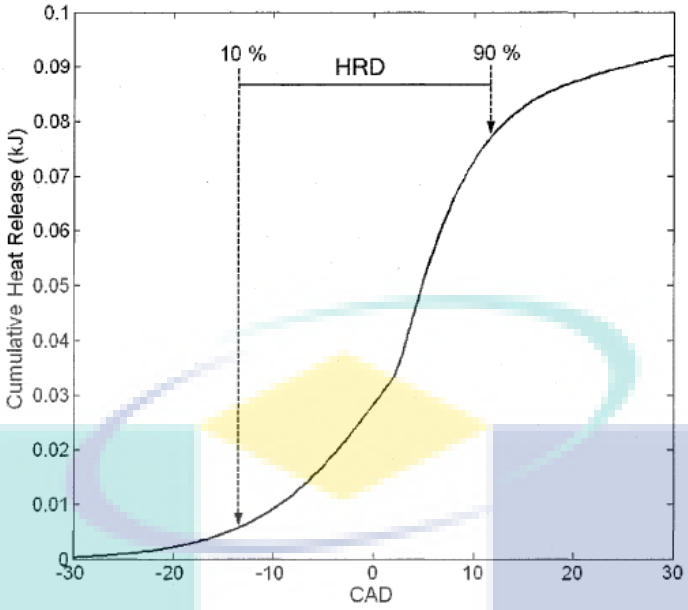

Figure 3.7 Process of determining SOC and combustion duration (CA10-90) (Mack [119])

The combustion duration (CA50) is often defined as the crank angle at which 50% of the cumulative heat release occurs. This is often referred to as CA50. Figure 3.8 graphically depicts this process.

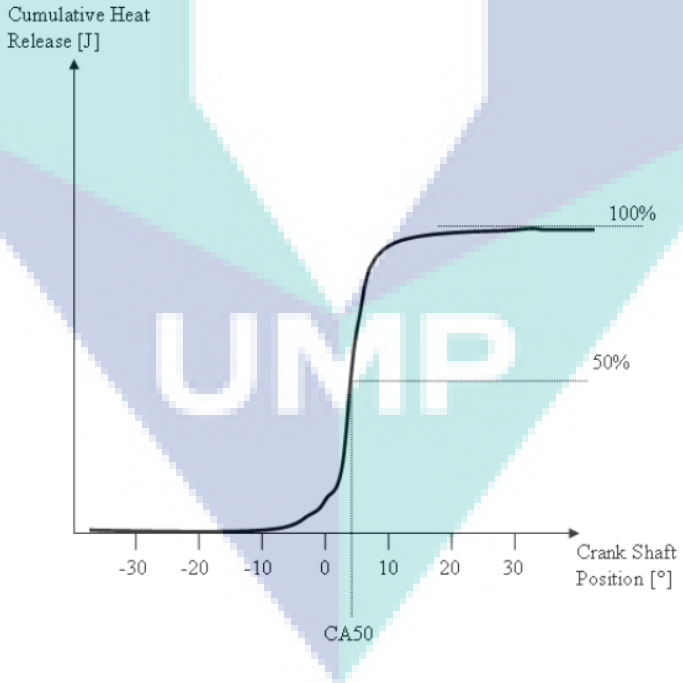

Figure 3.8 Process of determining CA50 (Hakansson [120])

3.4 Chemical Properties Of Fuels

In this study, different fuels are used in HCCI engines, including diesel, gasoline, *n*-heptane, ethanol, butanol and blends of *n*-heptane and ethanol as well as blends of *n*-heptane and butanol using 15% and 30% of both ethanol and butanol in blends. The properties of all test fuels are shown in Table 3.3, Table 3.4 and Table 3.5 respectively.

Table 3.3 The properties of diesel fuel (Guo, Hosseini [77])

Properties	Value
Chemical formula	C_7H_{16}
Density (kg/m^3)	679.5
Octane number	-----
Lower heating value (MJ/kg)	44.56
Boiling point(^{0}C)	98
Molar mass (g/mol)	100.16

Table 3.4 The properties of gasoline fuel (Gotoh, Kuboyama [51])

Properties	Value
Chemical formula	C_4-C_{12}
Density (kg/m^3)	747
Octane number	94
Lower heating value (MJ/kg)	44
Boiling point(^{0}C)	210

Table 3.5 The chemical properties of the test fuels (Holtzapple, Davison [121] and Saisirirat, Togbé [122])

Properties	n-hepatne	E15	E30	Bu15	Bu30
Chemical formula	C_7H_{16}	-	-	-	-
Density (kg/m^3)	679.5	697	713	700	808
Lower heating value (MJ/kg)	44.56	41	39	43	41
Boiling point(^{0}C)	98	95	92	101	117.7
Molar mass (g/mol)	100.16	92	84	96	74.12

4. RESULTS AND DISCUSSION

The validation of the zero-dimensional single zone model against the experimental results from the literature will be presented in this chapter. Two experimental data sets were used for validation purpose: one is the HCCI engine fuelled with diesel [117] and the other with gasoline [51]. This Chapter also presents the results of numerical modeling. The engine conditions including intake temperature, intake pressure, engine speed and the compression ratio will be varied to analyse the ability of the model to predict the combustion, performance and emissions characteristics of HCCI engines. The numerical results will be compared with experimental results from CI and SI engines to understand the advantages of HCCI engines over CI and SI engines. The use of fuel blends is an important concept for the HCCI engine. It helps to study the ability of HCCI engines to use a variety of fuels. This Chapter will describe the performance and emissions characteristics of HCCI engines and compare the results with CI and SI engines first. Then the effect of engine parameters on combustion and performance characteristics of both diesel and gasoline HCCI engines will be presented. After that, the effects of fuel blends in HCCI engines will be described. The summary will conclude the Chapter.

4.1 Model Validation of Diesel HCCI

In this section, the simulation models were validated by the experimental results that were conducted by Guo, Neill [117] on a four stroke single cylinder diesel engine which was modified for HCCI operation at a fixed engine speed of 900 rpm under the full engine load condition for diesel fuel. The detail specifications of the engines are presented in Table 4.1. The schematic diagram of the engine setup is presented in Figure 4.1.

Table 4.1 Engine model specifications (Guo, Neill [117])

Engine parameters	Value
Type	4 stroke, single cylinder
Bore (mm)	82.55
Stroke (mm)	114.3
Displacement (L)	0.6117
No. of cylinders	1
Compression ratio	4.6-16
Connecting rod length (mm)	254
Combustion chamber	Pancake shape
Intake Valve Close (°CA)	-144
Exhaust Valve Open (°CA)	140
Fuel system	Air-assist port fuel injection

The engine was modified from the standard ASTM guideline by the addition of an air-assist port fuel injection system and other hardware and software needed for the control of critical engine parameters such as intake air temperature, air/fuel ratio, exhaust gas recirculation and intake and exhaust back pressure. A port fuel injector for flexible fuel vehicles was modified to provide air-assist atomization of liquid fuels. Surge tanks were installed in the intake and exhaust systems to minimize pressure pulsations of the intake and exhaust gasses, thereby improving engine operational stability and airflow measurement. The low-speed data acquisition system is based on National Instruments' PXI hardware platform. The hardware is controlled by data acquisition and control software (Sakor Technologies, Inc., DynoLAB™ PT),

which provided stable control of the engine speed and load conditions, as well as critical parameters such as engine coolant and lubricating oil temperatures, intake air pressure and temperature, exhaust back pressure, fuel injection timing, and the quantity of fuel injected. The engine was coupled to an eddy current dynamometer that absorbed engine load. A variable-speed ac motor, coupled to the dynamometer with an overdrive clutch, was used to start and motor the engine before stable HCCI combustion was initiated, as well as to maintain engine speed when HCCI combustion was unstable.

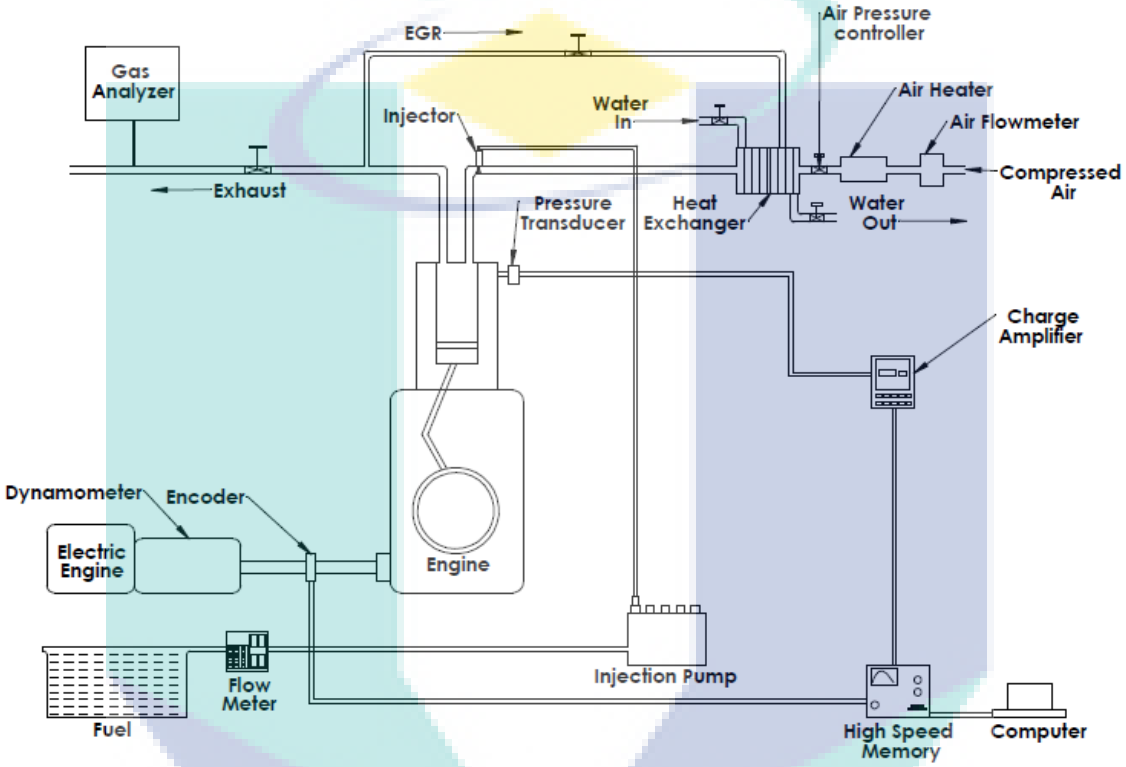

Figure 4.1 Schematic diagram of the HCCI engine set up, reproduced from [117]

In this study, the initial conditions for the intake pressure and temperature were set as P_{intake}=100 kPa and T_{intake}=333 K. The intake air temperature was set 20K higher than the actual temperature to account for the mixing effects [117]. A different study also stated that the intake temperature for a single-zone model has to be increased up to 30K, while up to about 10K for a multi-zone model [123]. The assumption of uniform wall temperature for the entire engine cycle, uniform in-cylinder temperature and pressure, and a potential limitation of the chemical chemistry as well may contribute to the adjustment of the intake temperature [117]. The wall temperature (T_{wall}) was set to be 530K for a CI engine [124]. However, the wall temperature used in the numerical studies varies from one engine to another [124-126], where the wall temperature ranges from 293K [127] to approximately 800K [125]. The exhaust temperature and pressure were approximated at 1000K and 101.3kPa, respectively [74], where the approximated value is close to measurement of a diesel engine [128]. At the beginning of the simulation, where CA is less than IVO, the mixture composition in the chamber was assumed to be only air with no fuel. The fuel is being introduced into the chamber during the IVO period, where the fuel quantity is based on the air-fuel ratio used in the experiment.

To further validate the applicability of the developed reaction mechanism for engine simulations, numerical simulations were performed and compared against the

HCCI engine experiments. The obtained results show good agreement with the experimental published results and capture important combustion phase trends as engine parameters are varied with a maximum percentage of error which is less than 6%. As presented in Figure 4.2, the numerical simulation was able to capture elements of HCCI combustion of diesel, particularly the low-temperature reaction (LTR). Figure 4.2(a) plots the in-cylinder pressure and Figure 4.2(b) plots the heat release rate obtained from experiments done by [117] and the present study, at a fixed engine speed of 900 rpm under constant intake temperature of 333 K and air-fuel ratio of 50 conditions.

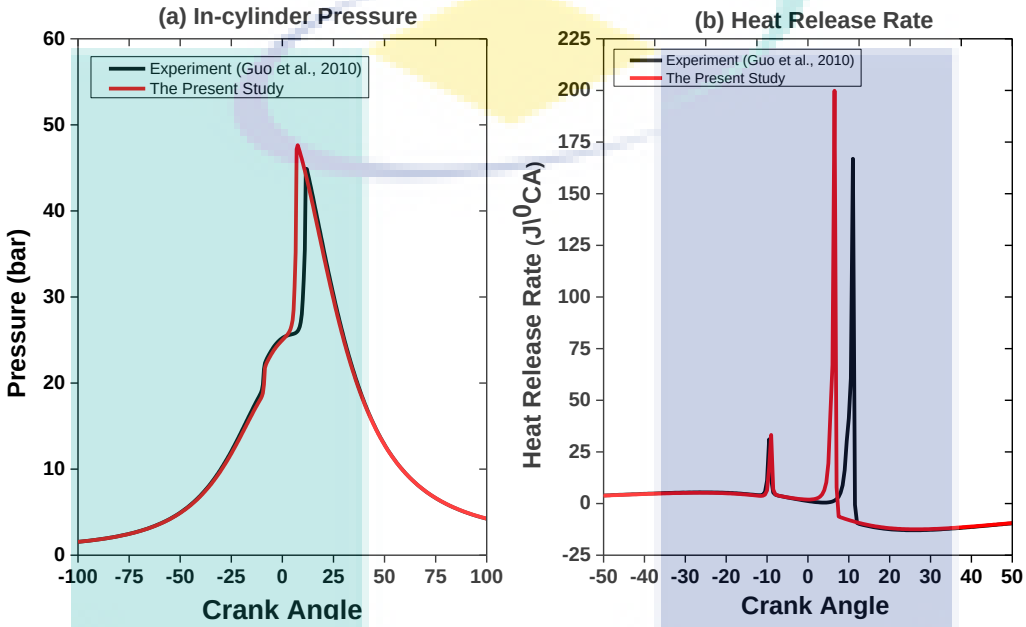

Figure 4.2 Comparison between zero-dimensional single zone model with experimental data [117]. CR=10, N=900 rpm, T_{in}=333 K, P_{in}=100 kPa, AFR=50

As can be seen, the peak cylinder pressure is adequately reproduced, indicating that the important reaction pathways are very well represented. In comparison, the main combustion stage (MCS) predicted by the numerical simulation is advanced compared to the experimental results as presented in Figure 4.2(b). A spike in the predicted heat release rate was observed during the MCS. This spike was caused by the rapid oxidation of all CO accumulated to this point in the simulation to CO_2 [129]. The conversion of CO to CO_2 is predicted to happen rapidly once the required temperature is reached because only a few reactions are involved. Rapid oxidation of CO to CO_2 has not been observed experimentally or reported in this study. The assumption of uniform mixture temperature and mixture composition contributes to this overly-rapid heat release rate.

2.2 Gasoline HCCI

In this section, the simulation models were validated by the experimental results that were conducted on a four stroke inline-4 cylinders gasoline engine which was modified for HCCI operation at a fixed engine speed of 1500 rpm under the full engine load condition for gasoline fuel surrogate. The detail specifications of the engines are presented in Table 4.2 [51]. The schematic diagram of the engine setup is presented in Figure 4.3. The engine was modified from the standard setup by the addition of hardware and software needed for the control of critical engine parameters such as intake air temperature, air-fuel ratio, exhaust gas recirculation and intake and

exhaust back pressure. The intake mean pressure was adjusted by varying the motor drive speed. The intake gas temperature was adjusted by a water-cooled intercooler. The partition ratio of a three-way valve was controlled to realize given intake temperature. The mean pressure in the exhaust pipe was controlled using an exhaust throttle valve. The cylinder pressure of the cylinder was measured by a piezoelectric pressure transducer (Kistler 6052c, 6117b). The crank angle of the 50% burn (CA50) was used to monitor the combustion phasing, and grossIMEP was used to recognize the output power of an individual cylinder. To balance the cylinder-to-cylinder variation of CA50 and grossIMEP, the amount of supplied fuel for the each cylinder were adjusted. All of the pressure analysis data including apparent HRR, mean effective pressures and pressure rise rate were computed from the ensemble-averaged pressure trace taken over 100 cycles. Piezo-resistive pressure transducers (Kistler 4005B) were mounted on the intake and the exhaust manifolds for the measurements of intake and exhaust pressure pulsations.

Table 4.2. Engine model specifications (Gotoh, Kuboyama [51])

Engine parameters	**Value**
Type	4 stroke, Inline-4 cylinder
Bore (mm)	86
Stroke (mm)	86
Displacement (L)	0.5
No. of cylinders	4
Compression ratio	12
Connecting rod length (mm)	200
Fuel	Gasoline (RON 91)
Intake Valve Close (°CA)	-180
Exhaust Valve Open (°CA)	156
Fuel system	Air-assist port fuel injection

In this study, the initial conditions for the intake pressure and temperature were set as P_{intake}=100 kPa and T_{intake}=393 K. The intake temperature for the zero-dimensional model was set 15°C higher than the actual to account for the mixing effects. This is consistent with Bunting, Eaton [123] and Guo, Neill [117], where the intake temperature for the zero-dimensional model was set 10 – 30 K higher than the actual. The wall temperature (T_{wall}) was set to be 353K which is consistent with Barroso, Escher [127] and Su, Mosbach [130]. However, the wall temperature used in the numerical studies varies from one engine to another [124-126], where the wall temperature ranges from 293K [127] to approximately 800K [125]. The exhaust temperature and pressure were approximated at 700K and 101.3kPa, respectively [74], where the approximated value is close to measurement of a gasoline engine [128]. At the beginning of the simulation, which is before the IVO, the mixture in the chamber was assumed to be only air and the fuel-air mixture was added according to the pre-set air-fuel ratio value after the IVO.

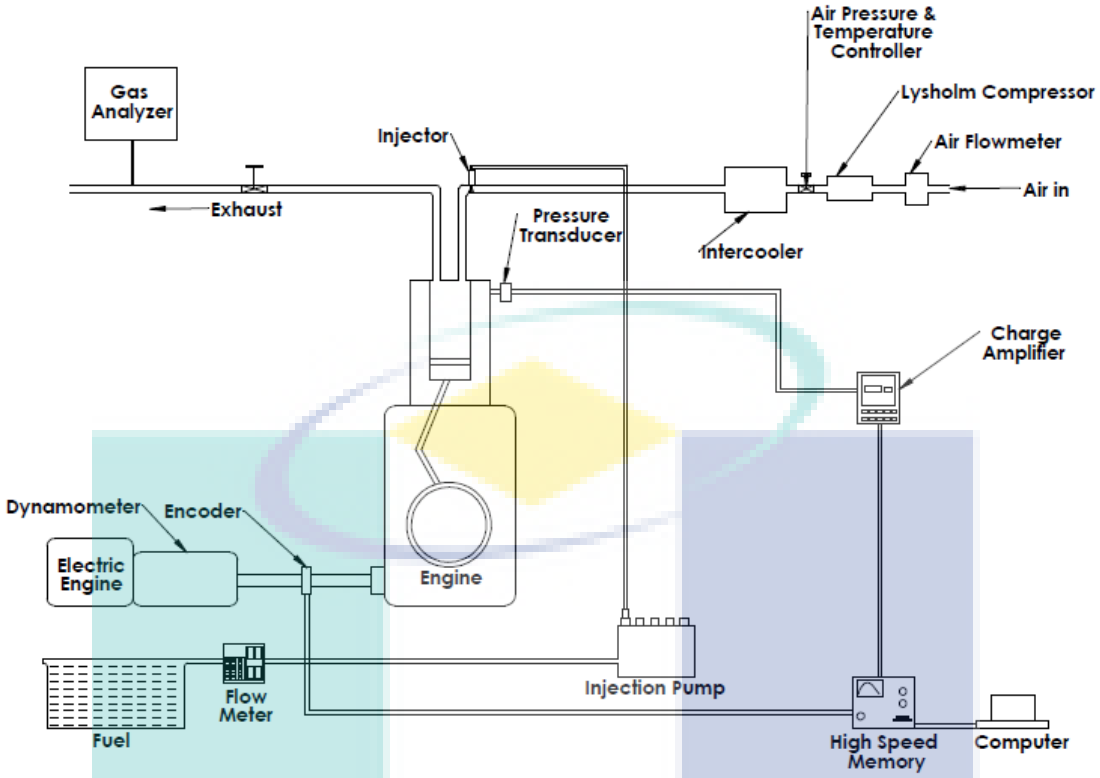

Figure 4.3 Schematic diagram of the HCCI engine set up, reproduced from [51]

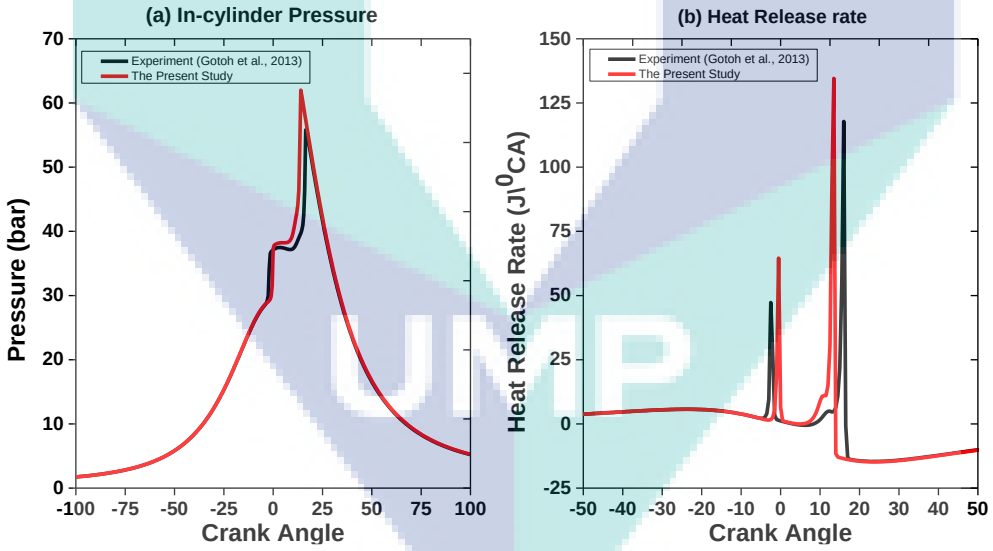

Figure 4.4 Comparison between zero-dimensional single zone model with experimental data [51]. CR=12, N=1500 rpm, T_{in}=393 K, P_{in}=100 kPa, AFR=40

To further validate the applicability of the developed reaction mechanism for engine simulations, numerical simulations were performed and compared against the HCCI engine experiments. The obtained results show good agreement with the experimental published results and capture important combustion phase trends as engine parameters are varied with maximum percentage of error which is less than 4%. As presented in Figure 4.4, the numerical simulation was able to capture elements of HCCI combustion of gasoline surrogate fuel, particularly the LTR. Figure 4.4(a) plots the in-cylinder pressure and Figure 4.4(b) plots the heat release rate obtained from experiments done by Gotoh, Kuboyama [51] and present study, at a fixed engine

speed of 1500 rpm under constant intake temperature of 393 K and air-fuel ratio of 40 conditions. As can be seen, the peak cylinder pressure is predicted higher than the experiment. The predicted maximum in-cylinder pressure is evidently slightly higher than that of the experiment due to the limitation of the zero-dimensional model, where the entire combustion chamber is assumed to be homogenous. In comparison, MCS predicted by the numerical simulation is advanced compared to the experimental data as presented in Figure 4.4(b). A spike in the predicted heat release rate was observed during the MCS. This spike was caused by the rapid oxidation of all CO accumulated to this point in the simulation to CO_2. The conversion of CO to CO_2 is predicted to happen rapidly once the required temperature is reached because only a few reactions are involved. The assumption of uniform mixture temperature and mixture composition contributes to this overly-rapid heat release rate. Overall, the combustion phasing is in good agreement with the experimental data, demonstrating that the zero-dimensional single-zone model can be used in HCCI engine simulations.

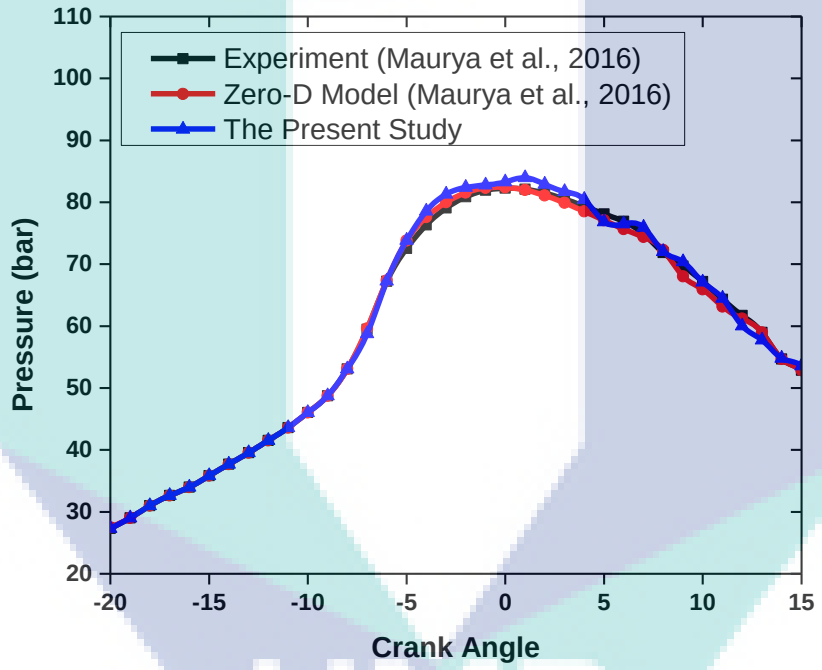

Figure 4.5 Comparison between zero-dimensional single zone model with experimental data and another zero-dimensional model [131]. CR=21, N=1000 rpm, T_{in}=365 K, P_{in}=100 kPa, λ = 3

4.3 Comparison of Different Models

In this section, the simulation results from the zero-dimensional single-zone model are compared with the experimental results as well as also compared with another zero-dimensional single-zone model from Maurya and Akhil [131] and one-dimensional model from Mo [132] as presented in Figures 4.5-4.6. From Figure 4.5, it is seen that both zero-dimensional models predict higher in-cylinder pressure compared to the experiment. While comparing between two zero-dimensional models, prediction of in-cylinder pressure from the zero-dimensional model of the present study is slightly better than the prediction from zero-dimensional of Maurya and Akhil [131]. The predicted maximum in-cylinder pressure is evidently slightly higher than that of the experiment due to the limitation of the zero-dimensional model, where the entire combustion chamber is assumed to be homogenous. From Figure 4.6, it is seen that the zero-dimensional model predicts the in-cylinder pressure properly. Very good agreement is seen between the experiment and simulation in terms of

combustion phasing and MCS prediction. While comparing between zero-dimensional model and one-dimensional model, prediction of in-cylinder pressure from a one-dimensional model of Mo [132] is slightly better than the prediction from zero-dimensional of the present study because of the prediction of knocking in a one-dimensional model. The reason behind this phenomenon is that the limitation of zero-dimensional modeling of assuming the whole combustion chamber is homogeneous. However, the combustion phasing is in good agreement with the simulation results of other types of numerical models, demonstrating that the zero-dimensional single-zone model of the present study can be used in HCCI engine simulations.

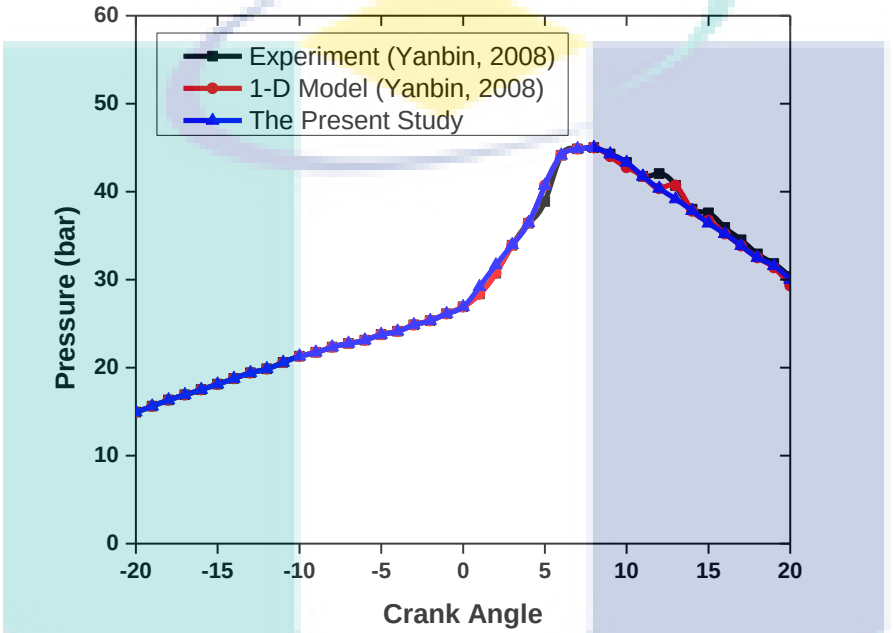

Figure 4.6 Comparison between zero-dimensional single zone model with experimental data and one-dimensional model [132]. CR=12, N=1995.7 rpm, T_{in}=388.96 K, P_{in}=93.99 kPa, λ = 1.5

2.3 Comparison of HCCI with CI

In this section, the comparison of performance and emissions characteristics between diesel and HCCI is discussed. The experimental performance and emissions characteristics for diesel engine using diesel fuel were done by An, Yang [129]. The detail specifications of the engines are presented in Table 4.3. The simulations were run for HCCI engine on same operating condition and using the same fuel.

4.3.1 Engine Performance

Figure 4.7 presents the variation of in-cylinder pressure between the diesel engine and HCCI engine at a constant speed of 2400 rpm and full load condition using diesel as a fuel. The in-cylinder pressure condition of the HCCI engine was selected at the best case condition of 333 K intake temperature when less knocking occurred. The in-cylinder pressure for the HCCI engine is higher than for the CI engine. The maximum pressure for the HCCI engine is 117 bar and 109.73 bar for the CI engine.

Table 4.3 Engine model specifications (An, Yang [129]).

Engine parameters	Value
Type	4 stroke, DI, water cooled
Bore (mm)	92
Stroke (mm)	93.8
Displacement (L)	0.6117
No. of cylinders	4
Compression ratio	18.5
Connecting rod length (mm)	158.5
Combustion chamber	Pancake shape
Intake Valve Close (°CA)	-144
Exhaust Valve Open (°CA)	140

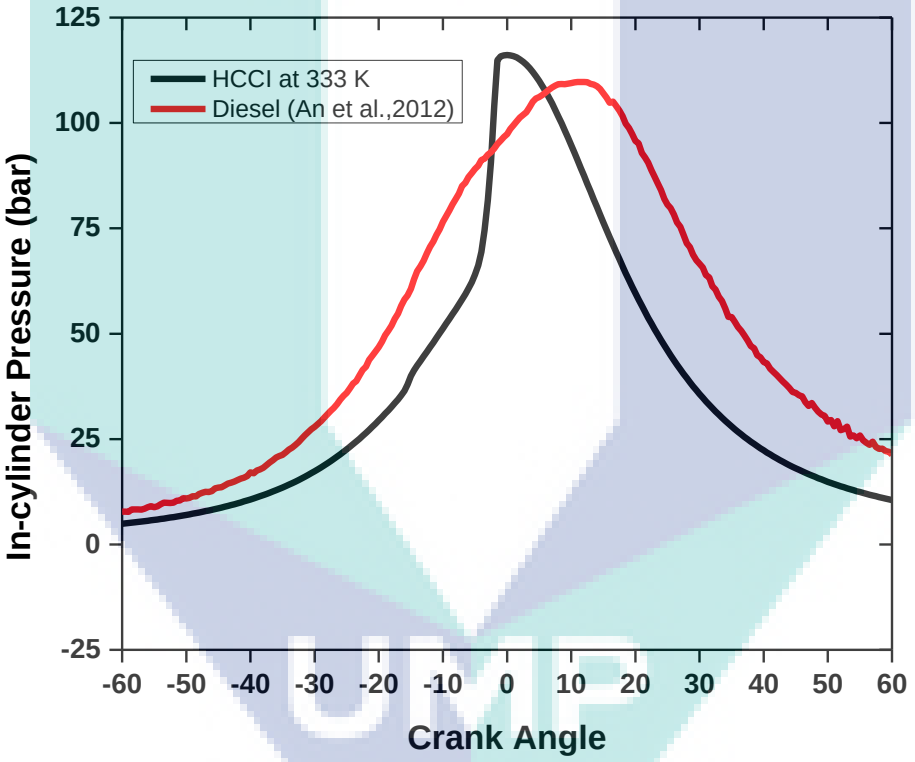

Figure 4.7 The variation of in-cylinder pressure between the diesel engine and HCCI engine at a constant speed of 2400 rpm and full load condition.

Note that from Figure 4.7 the combustion event for the HCCI engine occurs in a short time. The in-cylinder pressure increases faster and reaches a peak in approximately 8°CA with the combustion starting at 5°CA BTDC. With the CI engine, the pressure increases steadily and the combustion is slower compared to the HCCI engine. The combustion event for the CI engine starts at approximately 30°CA BTDC before the pressure reaches a peak at 10°CA ATDC. Thus, the combustion event for the CI engine occurred in approximately 40°CA, which is five times slower than for the HCCI. Hence, the combustion in the HCCI engine occurs instantaneously with very fast combustion, as has been discussed by Raitanapaibule and Aung [6] and Tomita [133]. Therefore, the HCCI combustion requires very well controlled

operating conditions to achieve the desired in-cylinder pressure behavior, otherwise knocking will take place.

Figure 4.8 presents the variation of engine power between the diesel engine and HCCI engine at a variable speed ranging from 1200 rpm to 3200 rpm and full load condition. It is seen that the HCCI engine power is higher than diesel engine in every speed condition except in 3200 rpm. The maximum power for the CI engine is 6.63 kW at 3200 rpm and 6.08 kW for the HCCI engine at 2800 rpm. An improvement in HCCI engine power was described in Figure 4.1, where the in-cylinder peak pressure is higher than CI engine. This improves the combustion efficiency which helps to increase power. In addition, the charge for HCCI engine is considered as homogeneous which is favorable for complete combustion. Thus combustion efficiency is improved and ultimately higher power is produced [134].

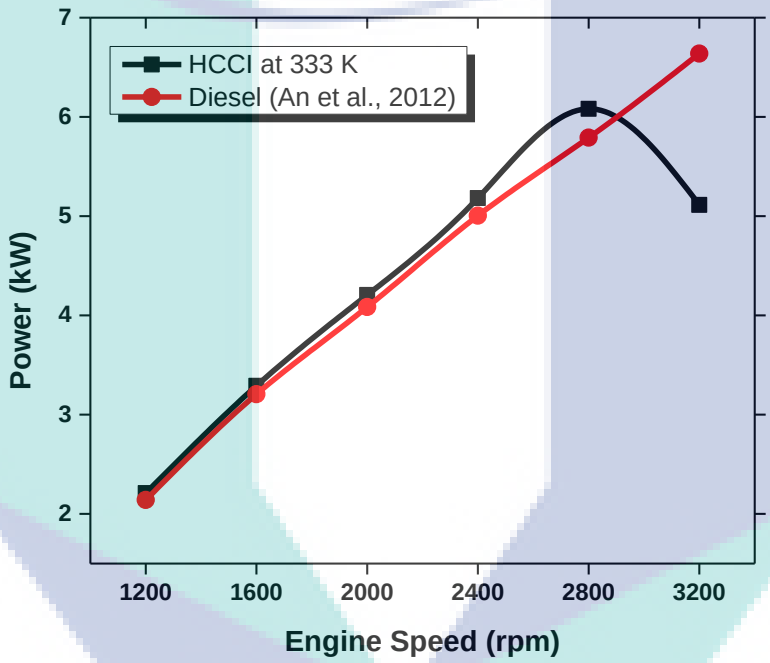

Figure 4.8 The variation of engine power between the diesel engine and HCCI engine at variable speed and full load condition.

Figure 4.9 presents the variation of BSFC between the diesel engine and HCCI engine at a variable speed ranging from 1200 rpm to 3200 rpm and full load condition. When compared with the HCCI engine, the BSFC for HCCI is better than the CI in every speed condition, as presented in Figure 4.3. The HCCI engine has the best BSFC at 215.64 g/kW-hr, where the CI has a minimum BSFC of 219.57 g/kW-hr. When the diesel engine operates in the highest speed condition, the BSFC marginally increases to 238.57 g/kW-hr. Thus, the HCCI engine has up to 1.65% lower BSFC than the diesel engine at the highest speed. This is because the power generated by the HCCI engine is higher due to the high compression ratio of the engine [135].

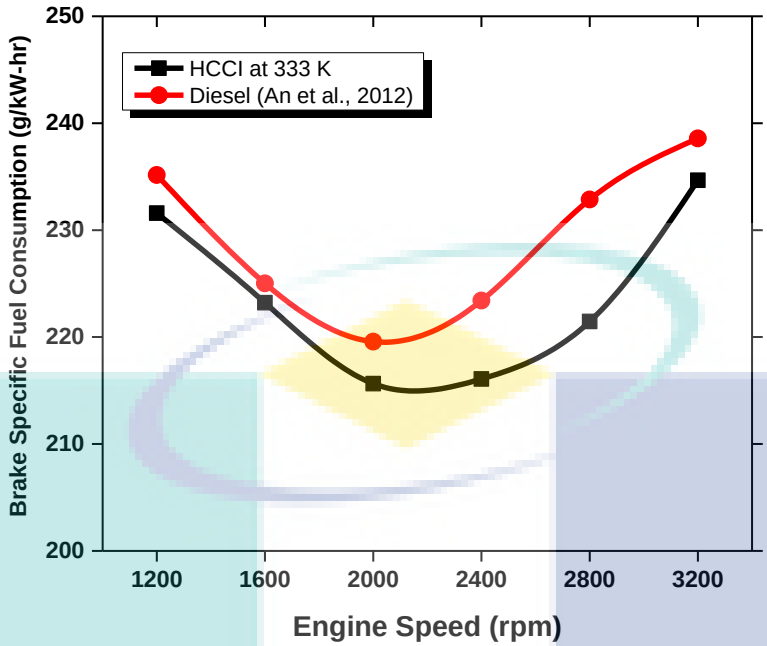

Figure 4.9 The variation of BSFC between the diesel engine and HCCI engine at variable speed and full load condition

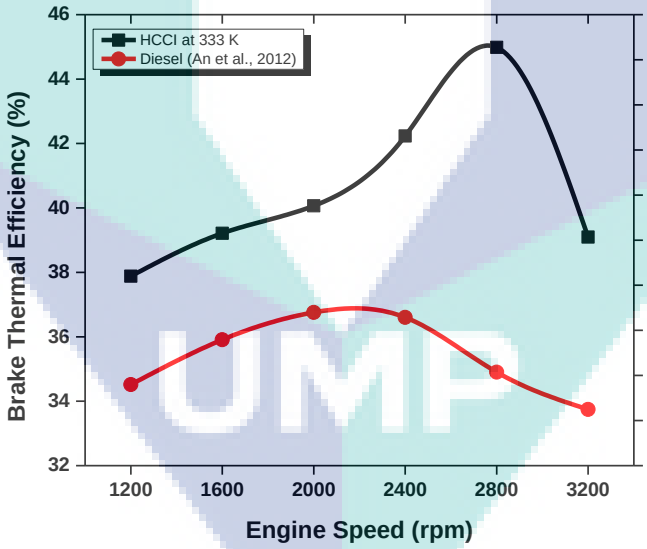

Figure 4.10 The variation of BTE between the diesel engine and HCCI engine at variable speed and full load condition.

Figure 4.10 presents the variation of BTE between the diesel engine and HCCI engine at a variable speed ranging from 1200 rpm to 3200 rpm and full load condition. It is seen that HCCI provides highest BTE at 2800 rpm whereas diesel engine provides at 2000 rpm. BTE of the HCCI engine increases with the increase of engine speed up to 2800 rpm and then decreases. When the BTE between the two modes of combustion is compared, the HCCI engine yields a higher efficiency than the diesel engine. The HCCI engine has a maximum efficiency of 44.98%, where the diesel engine has an efficiency of up to 36.75%. This is because the power generated by the HCCI engine is higher due to the high compression ratio of the engine [135].

4.3.2 Engine Emissions

Figure 4.11 presents the variation of HC emission between the diesel engine and HCCI engine at a variable speed ranging from 1200 rpm to 3200 rpm and full load condition. A significant difference in HC emission is seen between the diesel engine and the HCCI engine. This is one of the disadvantages of the HCCI engine which is already mentioned in the literature review. The HC emission from HCCI engine increases with the increase of engine speed up to 2400 rpm and then gradually decreases. When the HC emission between the two modes of combustion is compared, the HCCI engine yields a very higher amount of HC than the diesel engine. The HCCI engine has a maximum HC emission of 143 ppm, where the diesel engine has HC emission up to 9.94 ppm. This is due to the nature of this type of combustion. For low combustion temperature, incomplete combustion has occurred and ultimately HC emissions are produced [45, 82]. HC is mainly formed in the crevices of the cylinder which are so cold for complete consumption [75]. Higher concentrations of hydrogen and natural gas in diesel engines have the ability to reduce UHC and CO emission levels because the gaseous state of hydrogen and natural gas will reduce the wall wetting effect on the cylinder liner [83].

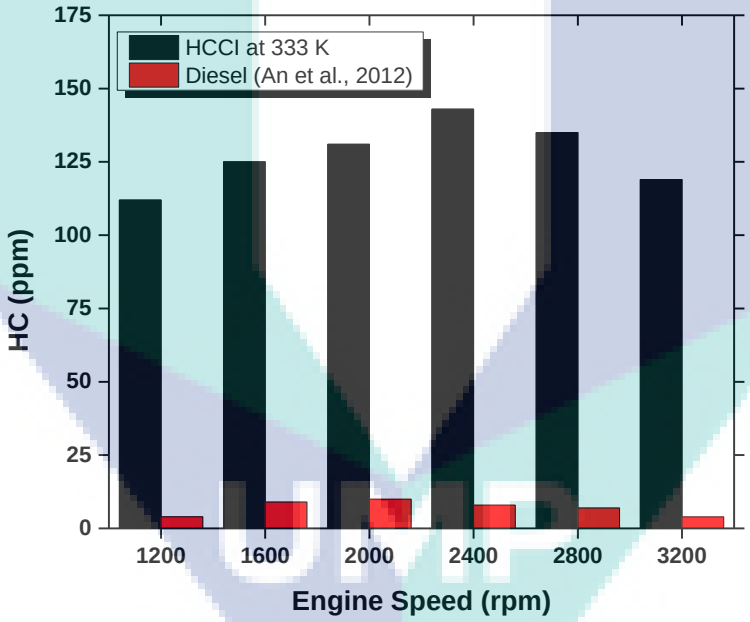

Figure 4.11 The variation of HC emission between the diesel engine and HCCI engine at variable speed and full load condition.

Figure 4.12 presents the variation of CO emission between the diesel engine and HCCI engine at a variable speed ranging from 1200 rpm to 3200 rpm and full load condition. A significant difference in CO emission is seen between the diesel engine and the HCCI engine. This is one of the disadvantages of the HCCI engine which is already mentioned in the literature review. When the HC emission between the two modes of combustion is compared, the HCCI engine yields a very higher amount of CO than the diesel engine. The HCCI engine has a maximum CO emission of 78 ppm, where the diesel engine has HC emission up to 4.22 ppm. This is due to the nature of this type of combustion. The amount of CO_2 and CO are dependent on the combustion efficiency, where the combustion efficiency can be defined as the ratio of CO_2 to the total of fuel carbon present in the exhaust including CO, CO_2 and

UHC [73]. CO is formed by following RH-R-RO2-RCHO-RCO-CO equation, where R is the hydrocarbon radical [74]. CO is mainly formed in the crevices of the cylinder which are so cold for complete consumption [75]. In addition, for the complete reaction of the conversion from CO to CO_2 needs temperature above 1500 K [76]. However, CO formation is occurred in case of HCCI combustion at low load peak burned gas temperature remains below that required level.

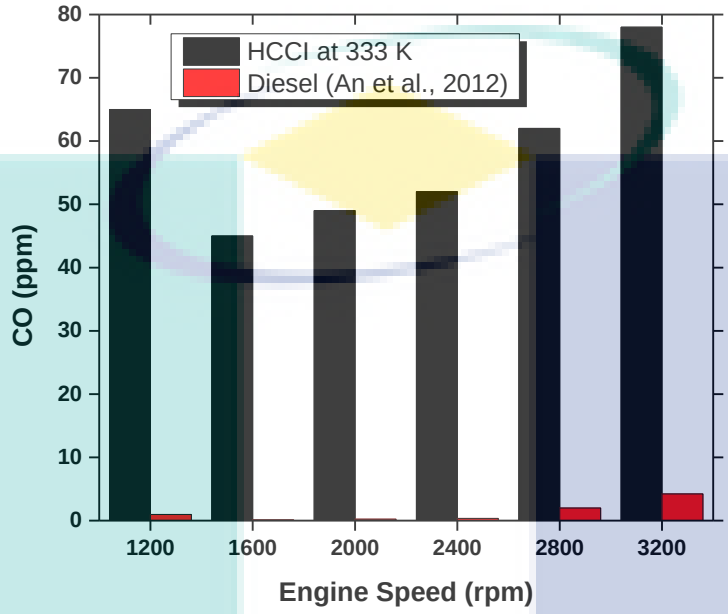

Figure 4.12 The variation of CO emission between the diesel engine and HCCI engine at variable speed and full load condition

Figure 4.13 presents the variation of NO_x emission between the diesel engine and HCCI engine at a variable speed ranging from 1200 rpm to 3200 rpm and full load condition. A significant difference in NO_x emission is seen between diesel engine and HCCI engine. This is one of the advantages of HCCI engine which is already mentioned in literature review. When the NO_x emission between the two modes of combustion is compared, the HCCI engine yields a very lower amount of NO_x than the diesel engine. The HCCI engine has a maximum NO_x emission of 10.8 ppm, where the diesel engine has NO_x emission up to 974.33 ppm. This is due to the nature of this type of combustion. The pollution formation process in CI engines is strongly dependent on fuel distribution system and the process of changing the distribution with time because of mixing. In case of diesel engines, fuel distribution system is non-uniform and the NO_x formation has occurred in the high temperature burned gas region which is non-uniform, as well as formation rates, are highest in this region close to stoichiometric ratio [74]. Since HCCI engines typically operate fuel lean, the final flame temperature is usually well below 2000 K. At this low post-combustion temperature chemical reactions that produce NO_x are essentially inactive [84]. NO_x is generally formed in a high temperature reaction, where the nitrogen in air dissociates into nitrogen radicals to form NO when reacting with oxygen. Some NO is converted to NO_2 when further reactions occur in the chamber.

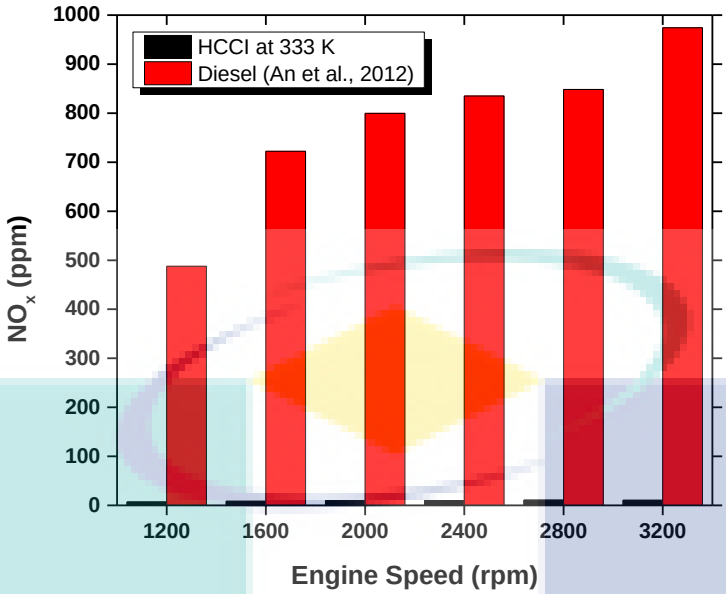

Figure 4.13 The variation of NO_x emission between the diesel engine and HCCI engine at variable speed and full load condition

3.5 Comparison of HCCI with SI

In this section, the comparison of performance and emissions characteristics between gasoline and HCCI is discussed. The experimental performance and emissions characteristics for gasoline engine using gasoline fuel surrogate were done by Topgül [136]. The detail specifications of the engines are presented in Table 4.4. The simulations were run for HCCI engine on same operating condition and using the same fuel.

Table 4.4 Engine model specifications [136].

Engine parameters	Value
Type	4 stroke, SI
Bore (mm)	80.26
Stroke (mm)	88.9
Displacement (L)	0.5117
No. of cylinders	1
Compression ratio	5.1-13.1
Connecting rod length (mm)	150
Intake Valve Close (°CA)	-144
Exhaust Valve Open (°CA)	140

4.4.1 Engine Performance

Figure 4.14 presents the variation of in-cylinder pressure between the gasoline engine and HCCI engine at a constant speed of 3000 rpm and full load condition using gasoline as a fuel. The in-cylinder pressure condition of the HCCI engine was selected at the best case condition of 393 K intake temperature when less knocking occurred. The in-cylinder pressure for the HCCI engine is higher than for the SI engine. The maximum pressure for the HCCI engine is 48.41 bar and 43.56 bar for the SI engine. It can be seen from Figure 4.14 that the combustion was happened in HCCI engine in a short time compared to SI engine. The combustion was started at 9°CA

BTDC and the in-cylinder pressure was increased faster and reached a peak approximately within 10°CA. On the other hand, combustion of SI engine was started at 14°CA BTDC and the in-cylinder pressure was increased slowly and reached the peak approximately within 30°CA which is three times slower than for the HCCI. Hence, the combustion in the HCCI engine occurs instantaneously with very fast combustion, as has been discussed by Raitanapaibule and Aung [6] and Tomita [133]. Therefore, the HCCI combustion requires very well controlled operating conditions to achieve the desired in-cylinder pressure behavior, otherwise knocking will take place.

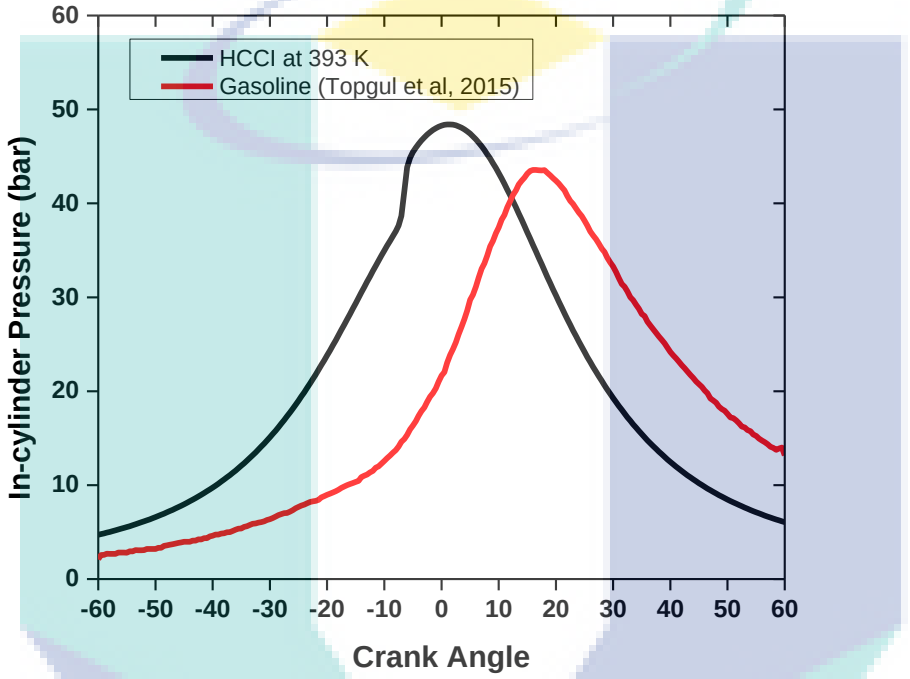

Figure 4.14. The variation of in-cylinder pressure between the gasoline engine and HCCI engine at a constant speed of 3000 rpm and full load condition

Figure 4.15 presents the variation of engine power between the gasoline engine and HCCI engine at a variable speed ranging from 1500 rpm to 4000 rpm and full load condition. From Figure 4.9 it is seen that the HCCI engine power is lower than the gasoline engine in every speed condition. The maximum power for the HCCI engine is 33 kW at 3500 rpm and 42.01 kW for the SI engine at 4000 rpm. A reduction in HCCI engine power was described in Figure 4.8, where the in-cylinder pressure trace experienced a rapid increase in pressure when combustion occurred. This, in turn, will reduce the area under the curve: meaning the work produced by the HCCI engine decreases. Integrating the in-cylinder pressure over the volume produces work. Hence, the work produced by the HCCI and SI engines by using the in-cylinder pressure in Figure 4.8 is 275.94 J and 299.80 J respectively. Thus, the HCCI engine produces less work than its SI counterpart, which translates into low power.

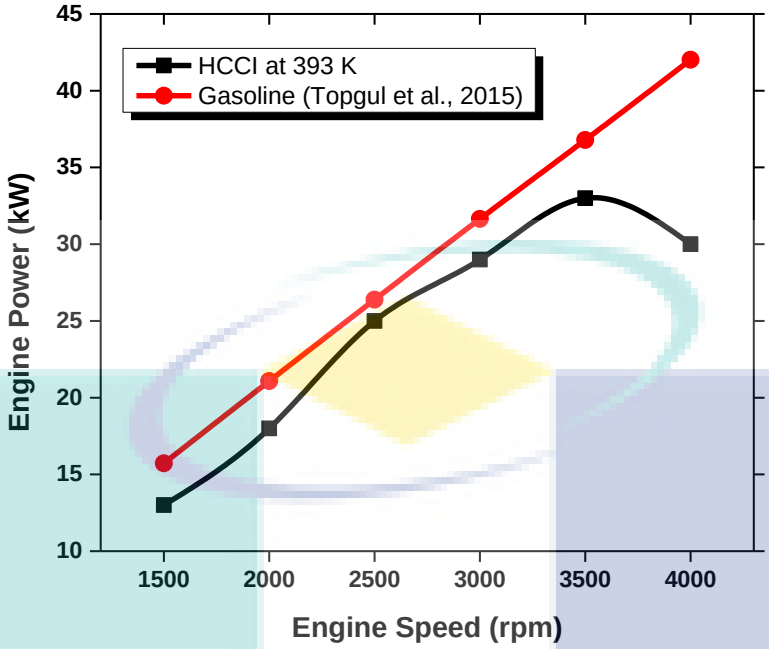

Figure 4.15 The variation of engine power between the gasoline engine and HCCI engine at variable speed and full load condition

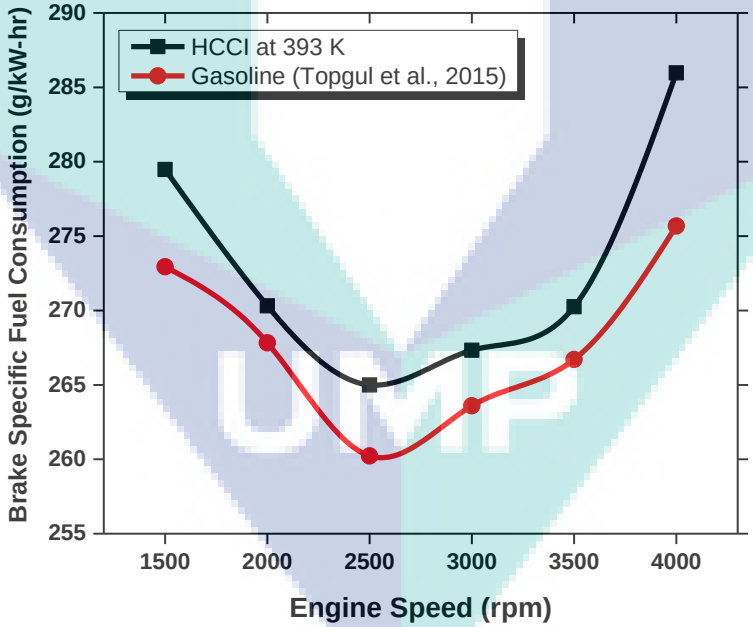

Figure 4.16 The variation of BSFC between the gasoline engine and HCCI engine at variable speed and full load condition.

Figure 4.16 presents the variation of BSFC between the gasoline engine and HCCI engine at a variable speed ranging from 1500 rpm to 4000 rpm and full load condition. When compared with the HCCI engine, the BSFC for HCCI is higher than the SI in every speed condition, as presented in Figure 4.10. The HCCI engine has the best BSFC at 264.99 g/kW-hr, where the SI has a minimum BSFC of 260.22 g/kW-hr. When the gasoline engine operates in the highest speed condition, the BSFC marginally increases to 275.68 g/kW-hr. Thus, the HCCI engine has up to 3.60% higher BSFC than the gasoline engine at the highest speed. This is because the power

generated by the HCCI engine is lower due to the low compression ratio of the engine. However, if the BSFC can be maintained lower than SI, the HCCI engine would be a good option shortly. The BSFC for the HCCI engine can be improved by using other parameters to control the combustion such as intake temperature, leaner mixture, exhaust gas recirculation etc.

Figure 4.17 presents the variation of BTE between the gasoline engine and HCCI engine at a variable speed ranging from 1500 rpm to 4000 rpm and full load condition. From Figure 4.17, it is seen that HCCI provides highest BTE at 3500 rpm whereas the gasoline engine provides at 2500 rpm. The HCCI engine BTE increases with the increase of engine speed up to 3500 rpm and then gradually decreases. When the BTE between the two modes of combustion is compared, the HCCI engine yields a lower efficiency than the gasoline engine. The HCCI engine has a maximum efficiency of 30.8%, where the gasoline engine has efficiency of up to 31.44%. This is because the power generated by the HCCI engine is lower due to the low compression ratio of the engine. Therefore, given a small difference in engine efficiency between gasoline and HCCI engines at the same operating condition, the HCCI engine can produce a better result if more tuning is carried out.

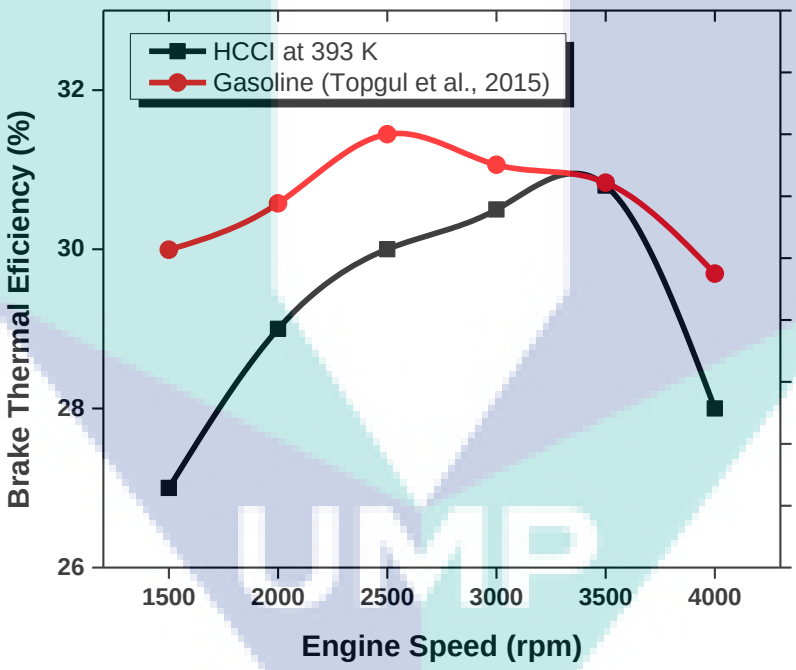

Figure 4.17 The variation of BTE between the gasoline engine and HCCI engine at variable speed and full load condition

4.4.2 Engine Emissions

Figure 4.18 presents the variation of HC emission between the gasoline engine and HCCI engine at a variable speed ranging from 1500 rpm to 4000 rpm and full load condition. A significant difference in HC emission is seen between the gasoline engine and the HCCI engine. The HC emission from HCCI engine decreases with the increase of engine speed. When the HC emission between the two modes of combustion is compared, the HCCI engine yields a very higher amount of HC than the gasoline engine. The HCCI engine has a maximum HC emission of 976 ppm, where the gasoline engine has HC emission up to 176.95 ppm. This is due to the nature of this type of combustion. For low combustion temperature, incomplete combustion is occurred and ultimately HC emissions is produced [45, 82]. HC is

mainly formed in the crevices of the cylinder which are so cold for complete consumption [75]. Higher concentrations of hydrogen and natural gas in gasoline engines have the ability to reduce UHC emission level, because the gaseous state of hydrogen and natural gas will reduce the wall wetting effect on the cylinder liner [83].

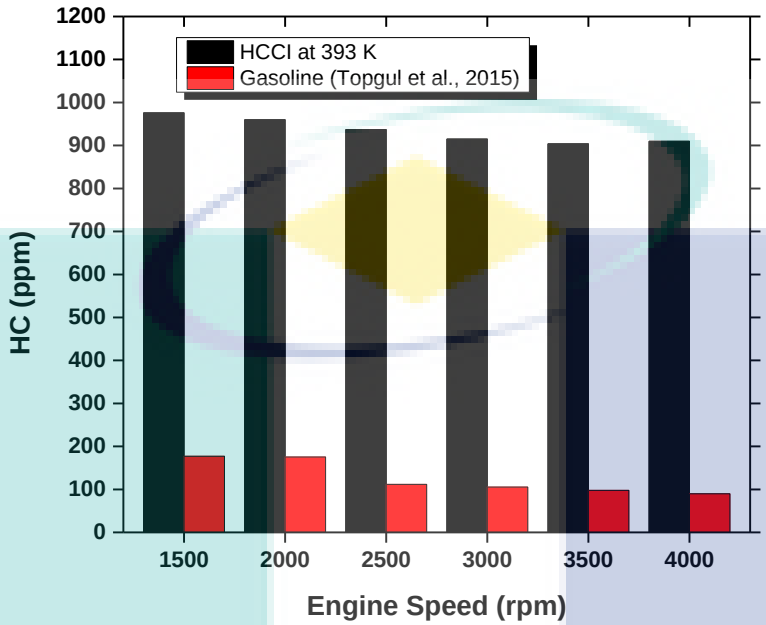

Figure 4.18. The variation of HC emission between the gasoline engine and HCCI engine at variable speed and full load condition.

Figure 4.19 presents the variation of CO emission between the gasoline engine and HCCI engine at a variable speed ranging from 1500 rpm to 4000 rpm and full load condition. A significant difference in CO emission is seen between the gasoline engine and the HCCI engine. This is one of the disadvantages of the HCCI engine which is already mentioned in the literature review. When the CO emission between the two modes of combustion is compared, the HCCI engine yields a very higher amount of CO than the gasoline engine. The HCCI engine has a maximum CO emission of 560 ppm, where the gasoline engine has HC emission up to 150 ppm. This is due to the nature of this type of combustion. The amount of CO_2 and CO are dependent on the combustion efficiency, where the combustion efficiency can be defined as the ratio of CO_2 to the total of fuel carbon present in the exhaust including CO, CO_2 and UHC [73]. CO is formed by following RH-R-RO2-RCHO-RCO-CO equation, where R is the hydrocarbon radical [74]. CO is mainly formed in the crevices of the cylinder which are so cold for complete consumption [75]. In addition, for the complete reaction of the conversion from CO to CO_2 needs temperature above 1500 K [76]. However, CO formation is occurred in case of HCCI combustion at low load peak burned gas temperature remains below that required level.

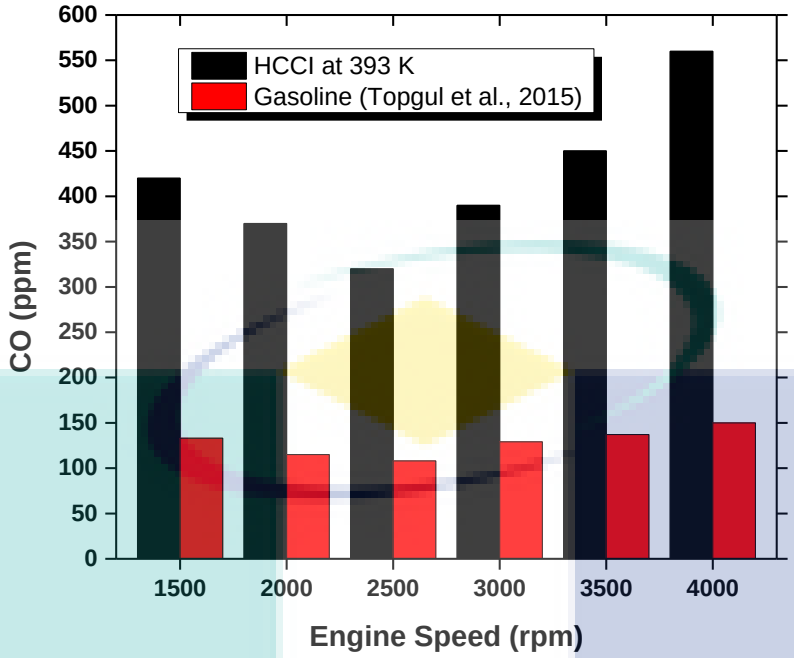

Figure 4.19 The variation of CO emission between the gasoline engine and HCCI engine at variable speed and full load condition.

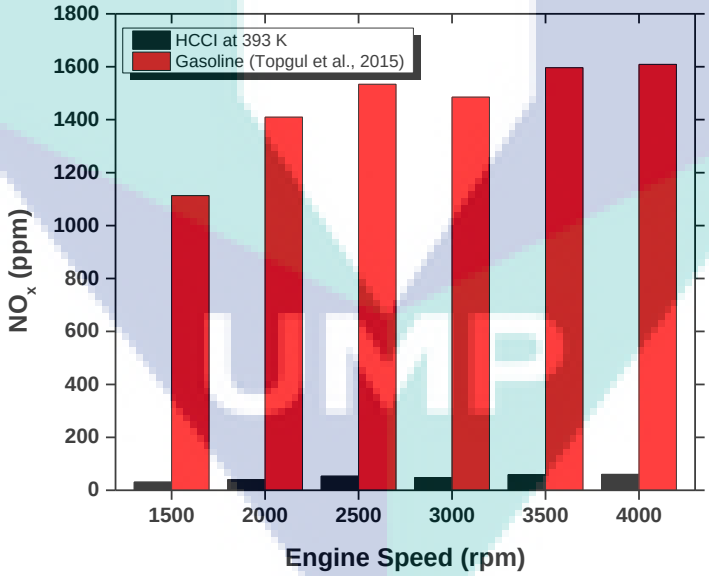

Figure 4.20 The variation of NO_x emission between the gasoline engine and HCCI engine at variable speed and full load condition.

Figure 4.20 presents the variation of NO_x emission between the gasoline engine and HCCI engine at a variable speed ranging from 1500 rpm to 4000 rpm and full load condition. A significant difference in NO_x emission is seen between the gasoline engine and the HCCI engine. This is one of the advantages of the HCCI engine which is already mentioned in the literature review. When the NO_x emission between the two modes of combustion is compared, the HCCI engine yields a very lower amount of NO_x than the gasoline engine. The HCCI engine has a maximum NO_x emission of 60 ppm, where the diesel engine has NO_x emission up to 1609.24 ppm. This is due to the nature of this type of combustion.

3. CONCLUSIONS AND RECOMMENDATIONS

In this study, a zero-dimensional single zone model was established to investigate HCCI combustion, performance and emissions characteristics over a wide range of operating conditions. Various chemical reaction mechanisms of various fuels and fuel blends were used to solve the chemical reactions during combustion. The model was validated against previously published experimental results. The simulations show good agreement with the experimental results and capture important combustion phase trends as engine parameters are varied with a maximum percentage of error which is less than 6% for diesel HCCI and 4% for gasoline HCCI. The validated numerical simulation was able to capture trends in combustion phasing variation with critical engine parameters, particularly the low-temperature reaction (LTR). The main combustion stage predicted by the numerical simulation is advanced compared to the experimental results because of the assumption of uniform mixture temperature and mixture composition.

This study reports the results of a modeling study of HCCI combustion using diesel fuel and compared the results with diesel engine experimental results using diesel fuel. When comparing the CI engines with HCCI engines at the same engine speed and load condition, CI engines have the advantage over the HCCI engine. This is consistent with the literature, where the HCCI engine has the limitation of operating in a low load condition. As for the emissions levels, the HCCI engine in this study recorded a very low level of NO_x due to the nature of this type of combustion. Unburned HC is higher than in the CI engines at full load condition. The same applies for CO emissions levels, where the HCCI engine returns higher CO than the CI engines at the same speed and load condition. This is also consistent with the literature where the HCCI engine has the disadvantage of producing more unburned HC and CO than the CI engines. Increasing the engine speed peak pressure location is retarded due to retarded MCS. IMEP, IT, and IP were increased up to a certain limit then decreased with increasing speed. This is because of with the increase of engine speed; the combustion duration is shortened with respect to time. Increasing the intake temperature advances the phasing of both the low-temperature reaction and main combustion stage and IMEP, IT and IP decreases with increasing intake temperature. This is due to the chemical reactions in the low-temperature phase which is retarded for increasing intake air temperature. The effects of turbocharging on the phasing of low-temperature reaction are relatively weak, but they significantly affect the phasing of the main combustion stage. The effect of compression ratio advances the phasing of the low-temperature reaction and main combustion stage and IMEP, IT and IP increases with increasing compression ratio.

This study also reports the results of a modeling study of HCCI combustion using gasoline surrogate fuel and compared the results with gasoline engine experimental results using gasoline surrogate fuel. When comparing the SI engines with HCCI engines at the same engine speed and load condition, SI engines have the advantage over the HCCI engine. This is consistent with the literature, where the HCCI engine has the limitation of operating in a low load condition. As for the emissions levels, the HCCI engine in this study recorded a very low level of NO_x due to nature of this type of combustion. Unburned HC is higher than in the SI engines at full load condition. The same applies for CO emissions levels, where the HCCI engine returns higher CO than the SI engines at the same speed and load condition. This is also consistent with the literature where the HCCI engine has the disadvantage of producing more unburned HC and CO than the SI engines. Increasing the engine speed peak pressure location is retarded due to retarded MCS. IMEP, IT, and IP were

increased up to a certain limit then decreased with increasing speed. This is because of with the increase in engine speed, the combustion duration is shortened with respect to time. Increasing the intake temperature advances the phasing of both the low-temperature reaction and main combustion stage and IMEP, IT and IP decreases with increasing intake temperature. This is due to the chemical reactions in the low-temperature phase which is retarded for increasing intake air temperature. The effects of turbocharging on the phasing of low-temperature reaction are relatively weak, but they significantly affect the phasing of the main combustion stage. The effect of compression ratio advances the phasing of the low-temperature reaction and main combustion stage and IMEP, IT and IP increases with increasing compression ratio. The model produced good agreement with the experiment but requires high computational resources. A zero-dimensional single-zone model has the advantage of faster computing time. However, it has the limitation of short burn duration which causes higher in-cylinder peak pressure. To mitigate this problem, a zero-dimensional single zone model can be developed to a one-dimensional single zone model. The use of a zero-dimensional single-zone model assumes that the combustion chamber is fully homogeneous without any turbulence effect. To mitigate this problem, a conditional momentum closure model can be added to a zero-dimensional single zone model.

REFERENCES

[1] Celik MB. Experimental determination of suitable ethanol–gasoline blend rate at high compression ratio for gasoline engine. Applied Thermal Engineering. 2008;28:396-404.

[2] Olsson J-O, Tunestål P, Johansson B, Fiveland S, Agama JR, Assanis DN. Compression ratio influence on maximum load of a natural gas fueled HCCI engine. SAE Transactions, Journal of Engines. 2002;111:442-58.

[3] Zhen X, Wang Y, Xu S, Zhu Y, Tao C, Xu T, et al. The engine knock analysis–An overview. Applied Energy. 2012;92:628-36.

[4] Lin Y-C, Hsu K-H, Chen C-B. Experimental investigation of the performance and emissions of a heavy-duty diesel engine fueled with waste cooking oil biodiesel/ultra-low sulfur diesel blends. Energy. 2011;36:241-8.

[5] Hasan M, Rahman M. Homogeneous charge compression ignition combustion: Advantages over compression ignition combustion, challenges and solutions. Renewable and Sustainable Energy Reviews. 2016;57:282-91.

[6] Raitanapaibule K, Aung K. Performance predictions of a hydrogen-enhanced natural gas HCCI engine. ASME 2005 International Mechanical Engineering Congress and Exposition: American Society of Mechanical Engineers; 2005. p. 289-94.

[7] Epping K, Aceves S, Bechtold R, Dec JE. The potential of HCCI combustion for high efficiency and low emissions. SAE Technical Paper; 2002.

[8] Kong S-C, Reitz RD. Use of detailed chemical kinetics to study HCCI engine combustion with consideration of turbulent mixing effects. Journal of engineering for gas turbines and power. 2002;124:702-7.

[9] Najt PM, Foster DE. Compression-ignited homogeneous charge combustion. SAE Technical paper; 1983.

[10] Killingsworth NJ, Aceves SM, Flowers DL, Krstić M. A simple HCCI engine model for control. Computer Aided Control System Design, 2006 IEEE International Conference on Control Applications, 2006 IEEE International Symposium on Intelligent Control, 2006 IEEE: IEEE; 2006. p. 2424-9.

[11] Mack JH, Aceves SM, Dibble RW. Demonstrating direct use of wet ethanol in a homogeneous charge compression ignition (HCCI) engine. Energy. 2009;34:782-7.
[12] Warnatz J, Maas U, Dibble RW. Combustion: physical and chemical fundamentals, modeling and simulation, experiments, pollutant formation: Springer; 2006.
[13] Kong S-C, Reitz RD. Numerical study of premixed HCCI engine combustion and its sensitivity to computational mesh and model uncertainties. Combustion Theory and Modelling. 2003;7:417-33.
[14] Gan S, Ng HK, Pang KM. Homogeneous charge compression ignition (HCCI) combustion: implementation and effects on pollutants in direct injection diesel engines. Applied Energy. 2011;88:559-67.
[15] Dang T, Teng J-t. The effects of configurations on the performance of microchannel counter-flow heat exchangers–An experimental study. Applied Thermal Engineering. 2011;31:3946-55.
[16] Zheng J, Yang W, Miller DL, Cernansky NP. Prediction of pre-ignition reactivity and ignition delay for HCCI using a reduced chemical kinetic model. SAE Technical Paper; 2001.
[17] Pucher GR, Gardiner DP, Bardon MF, Battista V. Alternative combustion systems for piston engines involving homogeneous charge compression ignition concepts-a review of studies using methanol, gasoline and diesel fuel. SAE Technical Paper; 1996.
[18] Zhao H. HCCI and CAI Engines for the Automotive Industry: Elsevier; 2007.
[19] Ericson C, Andersson M, Egnell R, Westerberg B. Modelling diesel engine combustion and NOx formation for model based control and simulation of engine and exhaust aftertreatment systems. SAE paper. 2006:0687.
[20] Soloiu V, Duggan M, Ochieng H, Williams D, Molina G, Vlcek B. Investigation of Low Temperature Combustion Regimes of Biodiesel With n-Butanol Injected in the Intake Manifold of a Compression Ignition Engine. Journal of Energy Resources Technology. 2013;135:041101.
[21] Miller JA, Bowman CT. Mechanism and modeling of nitrogen chemistry in combustion. Progress in energy and combustion science. 1989;15:287-338.
[22] Ishii H, Koike N, Suzuki H, Odaka M. Exhaust purification of diesel engines by homogeneous charge with compression ignition Part 2: Analysis of combustion phenomena and NOx formation by numerical simulation with experiment. SAE Technical Paper; 1997.
[23] Tree DR, Svensson KI. Soot processes in compression ignition engines. Progress in Energy and Combustion Science. 2007;33:272-309.
[24] Singh G, Singh AP, Agarwal AK. Experimental investigations of combustion, performance and emission characterization of biodiesel fuelled HCCI engine using external mixture formation technique. Sustainable Energy Technologies and Assessments. 2014;6:116-28.
[25] Jiménez-Espadafor FJ, Torres M, Velez JA, Carvajal E, Becerra JA. Experimental analysis of low temperature combustion mode with diesel and biodiesel fuels: A method for reducing NOx and soot emissions. Fuel Processing Technology. 2012;103:57-63.
[26] Ganesh D, Nagarajan G, Ganesan S. Experimental Investigation of Homogeneous Charge Compression Ignition Combustion of Biodiesel Fuel with External Mixture Formation in a CI engine. Environmental science & technology. 2014;48:3039-46.
[27] Canakci M. Combustion characteristics of a DI-HCCI gasoline engine running at different boost pressures. Fuel. 2012;96:546-55.

[28] Turkcan A, Ozsezen AN, Canakci M. Effects of second injection timing on combustion characteristics of a two stage direct injection gasoline–alcohol HCCI engine. Fuel. 2013;111:30-9.
[29] Ibrahim MM, Ramesh A. Investigations on the effects of intake temperature and charge dilution in a hydrogen fueled HCCI engine. International Journal of Hydrogen Energy. 2014;39:14097-108.
[30] Shi L, Cui Y, Deng K, Peng H, Chen Y. Study of low emission homogeneous charge compression ignition (HCCI) engine using combined internal and external exhaust gas recirculation (EGR). Energy. 2006;31:2665-76.
[31] García MT, Aguilar FJJ-E, Lencero TS, Villanueva JAB. A new heat release rate (HRR) law for homogeneous charge compression ignition (HCCI) combustion mode. Applied Thermal Engineering. 2009;29:3654-62.
[32] Singh AP, Agarwal AK. Combustion characteristics of diesel HCCI engine: an experimental investigation using external mixture formation technique. Applied Energy. 2012;99:116-25.
[33] Swami Nathan S, Mallikarjuna J, Ramesh A. Effects of charge temperature and exhaust gas re-circulation on combustion and emission characteristics of an acetylene fuelled HCCI engine. Fuel. 2010;89:515-21.
[34] Gomes Antunes J, Mikalsen R, Roskilly A. An investigation of hydrogen-fuelled HCCI engine performance and operation. International Journal of Hydrogen Energy. 2008;33:5823-8.
[35] Zhang S, Broadbelt LJ, Androulakis IP, Ierapetritou MG. Comparison of biodiesel performance based on HCCI engine simulation using detailed mechanism with on-the-fly reduction. Energy & Fuels. 2012;26:976-83.
[36] Kulzer A, Lejsek D, Nier T. A thermodynamic study on boosted HCCI: motivation, analysis and potential. SAE Technical Paper; 2010.
[37] Sjöberg M, Dec JE. Smoothing HCCI heat-release rates using partial fuel stratification with two-stage ignition fuels. SAE Technical Paper; 2006.
[38] Yang Y, Dec JE, Dronniou N, Sjöberg M. Tailoring HCCI heat-release rates with partial fuel stratification: Comparison of two-stage and single-stage-ignition fuels. Proceedings of the Combustion Institute. 2011;33:3047-55.
[39] Dec JE, Sjöberg M. Isolating the effects of fuel chemistry on combustion phasing in an HCCI engine and the potential of fuel stratification for ignition control. SAE Technical Paper; 2004.
[40] Garcia MT, Jiménez-Espadafor Aguilar FJ, Becerra Villanueva JA, Trujillo EC. Analysis of a new analytical law of heat release rate (HRR) for homogenous charge compression ignition (HCCI) combustion mode versus analytical parameters. Applied Thermal Engineering. 2011;31:458-66.
[41] Swami Nathan S, Mallikarjuna J, Ramesh A. An experimental study of the biogas–diesel HCCI mode of engine operation. Energy Conversion and Management. 2010;51:1347-53.
[42] Duc PM, Wattanavichien K. Study on biogas premixed charge diesel dual fuelled engine. Energy Conversion and Management. 2007;48:2286-308.
[43] Canakci M. An experimental study for the effects of boost pressure on the performance and exhaust emissions of a DI-HCCI gasoline engine. Fuel. 2008;87:1503-14.
[44] Ganesh D, Nagarajan G. Homogeneous charge compression ignition (HCCI) combustion of diesel fuel with external mixture formation. Energy. 2010;35:148-57.
[45] Ganesh D, Nagarajan G, Mohamed Ibrahim M. Study of performance, combustion and emission characteristics of diesel homogeneous charge compression ignition (HCCI) combustion with external mixture formation. Fuel. 2008;87:3497-503.

[46] Ma J, Lü X, Ji L, Huang Z. An experimental study of HCCI-DI combustion and emissions in a diesel engine with dual fuel. International Journal of Thermal Sciences. 2008;47:1235-42.
[47] Payri F, Lujan J, Martin J, Abbad A. Digital signal processing of in-cylinder pressure for combustion diagnosis of internal combustion engines. Mechanical Systems and Signal Processing. 2010;24:1767-84.
[48] Polovina D, McKenna D, Wheeler J, Sterniak J, Miersch-Wiemers O, Mond A, et al. Steady-state combustion development of a downsized multi-cylinder engine with range extended HCCI/SACI capability. SAE Technical Paper; 2013.
[49] Szybist JP, Edwards KD, Foster M, Confer K, Moore W. Characterization of engine control authority on HCCI combustion as the high load limit is approached. SAE Technical Paper; 2013.
[50] Ji C, Dec JE, Dernotte J, Cannella W. Effect of Ignition Improvers on the Combustion Performance of Regular-Grade E10 Gasoline in an HCCI Engine. SAE Technical Paper; 2014.
[51] Gotoh S, Kuboyama T, Moriyoshi Y, Hatamura K, Yamada T, Takanashi J, et al. Evaluation of the Performance of a Boosted HCCI Gasoline Engine with Blowdown Supercharge System. SAE Technical Paper; 2013.
[52] Zhang Y, Zhao H. Investigation of combustion, performance and emission characteristics of 2-stroke and 4-stroke spark ignition and CAI/HCCI operations in a DI gasoline. Applied Energy. 2014;130:244-55.
[53] Yap D, Karlovsky J, Megaritis A, Wyszynski M, Xu H. An investigation into propane homogeneous charge compression ignition (HCCI) engine operation with residual gas trapping. Fuel. 2005;84:2372-9.
[54] Kobayashi K, Sako T, Sakaguchi Y, Morimoto S, Kanematsu S, Suzuki K, et al. Development of HCCI natural gas engines. Journal of Natural Gas Science and Engineering. 2011;3:651-6.
[55] Milovanovic N, Blundell D, Pearson R, Turner J, Chen R. Enlarging the operational range of a gasoline HCCI engine by controlling the coolant temperature. 2005.
[56] Ghazikhani M, Feyz ME, Joharchi A. Experimental investigation of the Exhaust Gas Recirculation effects on irreversibility and Brake Specific Fuel Consumption of indirect injection diesel engines. Applied Thermal Engineering. 2010;30:1711-8.
[57] Zhuang Y, Hong G. Primary investigation to leveraging effect of using ethanol fuel on reducing gasoline fuel consumption. Fuel. 2013;105:425-31.
[58] Yun H, Wermuth N, Najt P. Extending the high load operating limit of a naturally-aspirated gasoline HCCI combustion engine. SAE Technical Paper; 2010.
[59] Al-Khairi NN, Naveenchandran P, Aziz ARA. Comparison of HCCI and SI Characteristics on Low Load CNG-DI Combustion. Applied Sci. 2011;11:1827-32.
[60] Kuboyama T, Moriyoshi Y, Hatamura K, Takanashi J, Urata Y. Extension of operating range of a multi-cylinder gasoline HCCI engine using the blowdown supercharging system. SAE Technical Paper; 2011.
[61] Lemberger I, Floweday G. 25cc HCCI Engine Fuelled with DEE. SAE Technical Paper; 2009.
[62] Hyvönen J, Haraldsson G, Johansson B. Operating conditions using spark assisted HCCI combustion during combustion mode transfer to SI in a multi-cylinder VCR-HCCI engine. SAE Technical Paper; 2005.
[63] He B-Q, Yuan J, Liu M-B, Zhao H. Combustion and emission characteristics of a n-butanol HCCI engine. Fuel. 2014;115:758-64.

[64] Machrafi H, Cavadias S, Amouroux J. A parametric study on the emissions from an HCCI alternative combustion engine resulting from the auto-ignition of primary reference fuels. Applied Energy. 2008;85:755-64.
[65] He B-Q, Liu M-B, Yuan J, Zhao H. Combustion and emission characteristics of a HCCI engine fuelled with n-butanol–gasoline blends. Fuel. 2013;108:668-74.
[66] Aceves SM, Flowers DL, Westbrook CK, Smith JR, Pitz W, Dibble R, et al. A multi-zone model for prediction of HCCI combustion and emissions. SAE Technical Paper; 2000.
[67] EPA-Gasoline R. Regulatory Impact Analysis—Control of Air Pollution from New Motor Vehicles: Tier 2 Motor Vehicle Emissions Standards and Gasoline Sulfur Control Requirements, US Environmental Protection Agency, Air and Radiation. US Environmental Protection Agency, Air and Radiation EPA420. 1999.
[68] Popp D. International innovation and diffusion of air pollution control technologies: the effects of NOx and SO_2 regulation in the US, Japan, and Germany. Journal of Environmental Economics and Management. 2006;51:46-71.
[69] Wesselink L, Buijsman E, Annema J. The impact of Euro 5: facts and figures. The Netherlands. 2006.
[70] Kong S-C, Reitz RD, Christensen M, Johansson B. Modeling the effects of geometry generated turbulence on HCCI engine combustion. SAE Technical Paper; 2003.
[71] Rizvi SQ. Lubricant Chemistry, Technology, Selection, and Design: West Conshohocken: ASTM International; 2009.
[72] Sanjid A, Masjuki H, Kalam M, Rahman S, Abedin M, Palash S. Impact of palm, mustard, waste cooking oil and< i> Calophyllum inophyllum</i> biofuels on performance and emission of CI engine. Renewable and Sustainable Energy Reviews. 2013;27:664-82.
[73] Li H, Neill WS, Chippior W, Graham L, Connolly T, Taylor JD. An experimental investigation on the emission characteristics of HCCI engine operation using n-heptane. SAE Technical Paper; 2007.
[74] Heywood JB. Internal combustion engine fundamentals: Mcgraw-hill New York; 1988.
[75] Aceves SM, Flowers DL, Martinez-Frias J, Smith JR, Dibble R, Au M, et al. HCCI combustion: analysis and experiments. SAE Technical Paper; 2001.
[76] Dec JE. A computational study of the effects of low fuel loading and EGR on heat release rates and combustion limits in HCCI engines. SAE Technical paper; 2002.
[77] Guo H, Hosseini V, Neill WS, Chippior WL, Dumitrescu CE. An experimental study on the effect of hydrogen enrichment on diesel fueled HCCI combustion. International journal of hydrogen energy. 2011;36:13820-30.
[78] Kim MY, Lee CS. Effect of a narrow fuel spray angle and a dual injection configuration on the improvement of exhaust emissions in a HCCI diesel engine. Fuel. 2007;86:2871-80.
[79] Yang F, Gao G, Ouyang M, Chen L, Yang Y. Research on a diesel HCCI engine assisted by an ISG motor. Applied Energy. 2013;101:718-29.
[80] Elghawi U, Mayouf A, Tsolakis A, Wyszynski M. Vapour-phase and particulate-bound PAHs profile generated by a (SI/HCCI) engine from a winter grade commercial gasoline fuel. Fuel. 2010;89:2019-25.
[81] Weall A, Szybist JP, Edwards KD, Foster M, Confer K, Moore W. HCCI load expansion opportunities using a fully variable HVA research engine to guide development of a production intent cam-based VVA engine: the low load limit. SAE Technical Paper; 2012.

[82] Bression G, Soleri D, Savy S, Dehoux S, Azoulay D, Hamouda HB-H, et al. A study of methods to lower HC and CO emissions in diesel HCCI. SAE Technical Paper; 2008.
[83] Cho HM, He B-Q. Spark ignition natural gas engines—A review. Energy Conversion and Management. 2007;48:608-18.
[84] Mack JH. Investigation of Homogeneous Charge Compression Ignition (HCCI) engines fuelled with ethanol blends using experiments and numerical simulations. PhD thesis. 2007.
[85] Tanaka S, Ayala F, Keck JC. A reduced chemical kinetic model for HCCI combustion of primary reference fuels in a rapid compression machine. Combustion and Flame. 2003;133:467-81.
[86] Komninos NP. Investigating the importance of mass transfer on the formation of HCCI engine emissions using a multi-zone model. Applied Energy. 2009;86:1335-43.
[87] Lu X-C, Chen W, Huang Z. A fundamental study on the control of the HCCI combustion and emissions by fuel design concept combined with controllable EGR. Part 2. Effect of operating conditions and EGR on HCCI combustion. Fuel. 2005;84:1084-92.
[88] Machrafi H, Cavadias S, Amouroux J. Influence of fuel type, dilution and equivalence ratio on the emission reduction from the auto-ignition in an Homogeneous Charge Compression Ignition engine. Energy. 2010;35:1829-38.
[89] Akagawa H, Miyamoto T, Harada A, Sasaki S, Shimazaki N, Hashizume T, et al. Approaches to solve problems of the premixed lean diesel combustion. SAE Technical Paper; 1999.
[90] Choi D, Miles PC, Yun H, Reitz RD. A parametric study of low-temperature, late-injection combustion in a HSDI diesel engine. JSME International Journal Series B Fluids and Thermal Engineering. 2005;48:656-64.
[91] Christensen M, Johansson B, Amnéus P, Mauss F. Supercharged homogeneous charge compression ignition. SAE Transactions, Journal of Engines. 1998;107.
[92] Christensen M, Johansson B. Supercharged homogeneous charge compression ignition (HCCI) with exhaust gas recirculation and pilot fuel. SAE Technical Paper; 2000.
[93] Hyvönen J, Haraldsson G, Johansson B. Supercharging HCCI to extend the operating range in a multi-cylinder VCR-HCCI engine. SAE paper. 2003:3214.
[94] Iwabuchi Y, Kawai K, Shoji T, Takeda Y. Trial of new concept diesel combustion system-premixed compression-ignited combustion. SAE Technical Paper; 1999.
[95] Hosseini V, Checkel MD. Intake pressure effects on HCCI combustion in a CFR engine. Proceedings of the combustion institute, canadian section, spring technical meeting2007.
[96] Olsson J-O, Tunestål P, Haraldsson G, Johansson B. A turbocharged dual-fuel HCCI engine. SAE Special Publications. 2001;2001.
[97] Olsson J-O, Tunestål P, Johansson B. Boosting for high load HCCI. SAE Technical Paper; 2004.
[98] Raheman H, Phadatare A. Diesel engine emissions and performance from blends of karanja methyl ester and diesel. Biomass and Bioenergy. 2004;27:393-7.
[99] Peng Z, Zhao H, Ma T, Ladommatos N. Characteristics of homogeneous charge compression ignition (HCCI) combustion and emissions of n-heptane. Combustion science and technology. 2005;177:2113-50.
[100] Laguitton O, Crua C, Cowell T, Heikal M, Gold M. The effect of compression ratio on exhaust emissions from a PCCI diesel engine. Energy Conversion and Management. 2007;48:2918-24.

[101] Pei Y, Mehl M, Liu W, Lu T, Pitz WJ, Som S. A Multicomponent Blend as a Diesel Fuel Surrogate for Compression Ignition Engine Applications. Journal of Engineering for Gas Turbines and Power. 2015;137:111502.
[102] Sarathy SM, Westbrook CK, Mehl M, Pitz WJ, Togbe C, Dagaut P, et al. Comprehensive chemical kinetic modeling of the oxidation of 2-methylalkanes from C 7 to C 20. Combustion and flame. 2011;158:2338-57.
[103] Lu T, Plomer M, Luo Z, Sarathy S, Pitz W, Som S, et al. Directed relation graph with expert knowledge for skeletal mechanism reduction. 7th US national combustion meeting, Atlanta, GA2011.
[104] Mehl M, Chen J-Y, Pitz WJ, Sarathy S, Westbrook CK. An approach for formulating surrogates for gasoline with application toward a reduced surrogate mechanism for CFD engine modeling. Energy & Fuels. 2011;25:5215-23.
[105] Mehl M, Pitz WJ, Westbrook CK, Curran HJ. Kinetic modeling of gasoline surrogate components and mixtures under engine conditions. Proceedings of the Combustion Institute. 2011;33:193-200.
[106] Mehl M, Pitz W, Sarathy M, Yang Y, Dec JE. Detailed kinetic modeling of conventional gasoline at highly boosted conditions and the associated intermediate temperature heat release. SAE Technical Paper; 2012.
[107] Dec JE, Yang Y. Boosted HCCI for high power without engine knock and with ultra-low NOx emissions-using conventional gasoline. SAE International Journal of Engines. 2010;3:750-67.
[108] Seiser R, Pitsch H, Seshadri K, Pitz W, Gurran H. Extinction and autoignition of n-heptane in counterflow configuration. Proceedings of the Combustion Institute. 2000;28:2029-37.
[109] Dagaut P, Togbé C. Experimental and modeling study of the kinetics of oxidation of ethanol-n-heptane mixtures in a jet-stirred reactor. Fuel. 2010;89:280-6.
[110] Dagaut P, Togbé C. Experimental and modeling study of the kinetics of oxidation of butanol− n-heptane mixtures in a jet-stirred reactor. Energy & Fuels. 2009;23:3527-35.
[111] Golub A, Ghoniem A. Modeling NOx formation in a small bore, lean natural gas, spark ignition engine. SAE Technical Paper; 1999.
[112] Amnéus P, Mauss F, Kraft M, Vressner A, Johansson B. NOx and N2O formation in HCCI engines. SAE Technical Paper; 2005.
[113] Miller JA, Pilling MJ, Troe J. Unravelling combustion mechanisms through a quantitative understanding of elementary reactions. Proceedings of the Combustion Institute. 2005;30:43-88.
[114] Mueller MA, Yetter RA, Dryer FL. Kinetic modeling of the CO/H2O/O2/NO/SO2 system: Implications for high-pressure fall-off in the SO2 + O(+M) = SO3(+M) reaction. International Journal of Chemical Kinetics. 2000;32:317-39.
[115] Shaver GM, Gerdes JC, Jain P, Caton P, Edwards C. Modeling for control of HCCI engines. American Control Conference, 2003 Proceedings of the 2003: IEEE; 2003. p. 749-54.
[116] Canova M, Garcin R, Midlam-Mohler S, Guezennec Y, Rizzoni G. A control-oriented model of combustion process in a HCCI diesel engine. American Control Conference, 2005 Proceedings of the 2005: IEEE; 2005. p. 4446-51.
[117] Guo H, Neill WS, Chippior W, Li H, Taylor JD. An experimental and modeling study of HCCI combustion using n-heptane. Journal of Engineering for Gas Turbines and Power. 2010;132:022801.
[118] Andrae J. A kinetic modeling study of self-ignition of low alkylbenzenes at engine-relevant conditions. Fuel Processing Technology. 2011;92:2030-40.

[119] Mack JH. Investigation of homogeneous charge compression ignition (HCCI) engines fuelled with ethanol blends using experiments and numerical simulations: University of California, Berkeley; 2007.
[120] Hakansson A. CA50 estimation on HCCI engine using engine speed variations. Lund University: MSc Thesis. 2007.
[121] Holtzapple MT, Davison RR, Ross MK, Aldrett-Lee S, Nagwani M, Lee C-M, et al. Biomass conversion to mixed alcohol fuels using the MixAlco process. Twentieth Symposium on Biotechnology for Fuels and Chemicals: Springer; 1999. p. 609-31.
[122] Saisirirat P, Togbé C, Chanchaona S, Foucher F, Mounaim-Rousselle C, Dagaut P. Auto-ignition and combustion characteristics in HCCI and JSR using 1-butanol/n-heptane and ethanol/n-heptane blends. Proceedings of the Combustion Institute. 2011;33:3007-14.
[123] Bunting BG, Eaton S, Naik CV, Puduppakkam KV, Chou C-P, Meeks E. A Comparison of HCCI Ignition Characteristics of Gasoline Fuels Using a Single-Zone Kinetic Model with a Five Component Surrogate Fuel. SAE Technical Paper; 2008.
[124] Zheng QP, Zhang HM. A computational study of combustion in compression ignition natural gas engine with separated chamber. Fuel. 2005;84:1515-23.
[125] Soyhan H, Yasar H, Walmsley H, Head B, Kalghatgi G, Sorusbay C. Evaluation of heat transfer correlations for HCCI engine modeling. Applied Thermal Engineering. 2009;29:541-9.
[126] Wang Z, Shuai S-J, Wang J-X, Tian G-H, An X-L. Modeling of HCCI combustion: From 0D to 3D. SAE Technical Paper; 2006.
[127] Barroso G, Escher A, Boulouchos K. Experimental and numerical investigations on HCCI-combustion. 7th International Conference on Engines for Automobile: Citeseer; 2005.
[128] Zhou P, Zhou S, Clelland D. A modified quasi-dimensional multi-zone combustion model for direct injection diesels. International Journal of Engine Research. 2006;7:335-45.
[129] An H, Yang W, Chou S, Chua K. Combustion and emissions characteristics of diesel engine fueled by biodiesel at partial load conditions. Applied Energy. 2012;99:363-71.
[130] Su H, Mosbach S, Kraft M, Bhave A, Kook S, Bae C. Two-stage fuel direct injection in a diesel fuelled HCCI engine. SAE paper. 2007:01-1880.
[131] Maurya RK, Akhil N. Numerical investigation of ethanol fuelled HCCI engine using stochastic reactor model. Part 2: Parametric study of performance and emissions characteristics using new reduced ethanol oxidation mechanism. Energy Conversion and Management. 2016;121:55-70.
[132] Mo Y. HCCI Heat Release Rate and Combustion Efficiency: A Couple KIVA Multi-Zone Modeling Study: ProQuest; 2008.
[133] Tomita E. Dual fuel HCCI combustion-High octane and high cetane number fuels. HCCI Symposium2004.
[134] Kook S, Bae C, Kim J. Diesel-fuelled homogeneous charge compression ignition engine with optimized premixing strategies. International Journal of Engine Research. 2007;8:127-37.
[135] Fiveland SB, Assanis DN. A four-stroke homogeneous charge compression ignition engine simulation for combustion and performance studies. Ann Arbor. 2000;1001:48108.
[136] Topgül T. The effects of MTBE blends on engine performance and exhaust emissions in a spark ignition engine. Fuel Processing Technology. 2015;138:483-9.